

Phase Transition Analysis for Covariance Based Massive Random Access with Massive MIMO

Zhilin Chen, Foad Sahrabi, Ya-Feng Liu, and Wei Yu

Abstract—This paper considers the massive random access problem in which a large number of sporadically active devices wish to communicate with a base-station (BS) equipped with a large number of antennas. Each device is preassigned a unique signature sequence, and the BS identifies the active devices in the random access by detecting which sequences are transmitted. This device activity detection problem can be formulated as a maximum likelihood estimation (MLE) problem with the sample covariance matrix of the received signal being a sufficient statistic. The aim of this paper is to characterize the parameter space in which this covariance based approach would be able to successfully recover the device activities in the massive multiple-input multiple-output (MIMO) regime. Through an analysis of the asymptotic behaviors of MLE via its associated Fisher information matrix, this paper derives a necessary and sufficient condition on the Fisher information matrix to ensure a vanishing detection error rate as the number of antennas goes to infinity, based on which a numerical phase transition analysis is obtained. This condition is also examined from a perspective of covariance matching that relates the phase transition analysis in this paper to a recently derived scaling law. Furthermore, this paper provides a characterization of the distribution of the estimation error in MLE, based on which the error probabilities in device activity detection can be accurately predicted. Finally, this paper studies a random access scheme with joint device activity and data detection and analyzes its performance in a similar way. Simulation results validate the analysis.

Index Terms—Device activity detection, Fisher information matrix, massive MIMO, massive machine-type communication (mMTC), massive random access, phase transition analysis

I. INTRODUCTION

Uncoordinated random access is a challenging task for massive machine-type communications (mMTC), in which a large number of sporadically active devices attempt to communicate with the base-station (BS) in the uplink [3]–[5]. Conventional cellular systems provide random access for human-type communications by employing a set of orthogonal sequences, from which every active device randomly and independently selects one sequence to transmit as a pilot for

requesting access [6]. When the number of active devices is comparable to the number of available orthogonal sequences, this uncoordinated random access approach inevitably leads to collisions. A subsequent collision-resolution mechanism is needed at the cost of delay due to the required multiple rounds of signaling. Such a scheme may not be suitable for mMTC due to the fact that the delay caused by contention resolution can be severe [7].

The issue of collision in random access for mMTC can be avoided by using non-orthogonal sequences [8]. The basic idea is to use a large set of non-orthogonal sequences and to preassign a unique pilot sequence to each device, then let all the active devices transmit their pilots simultaneously as identifiers. The BS can take advantage of the sporadic nature of the device activity pattern and use a sparse recovery (i.e., compressed sensing) algorithm to detect which sequences are transmitted, thereby identifying the active devices.

The ability to perform sparse recovery can be greatly enhanced if the BS is equipped with a large number of antennas. This is because the non-orthogonality of the pilot sequences leads to significant interference between the pilots, and a massive multiple-input multiple-output (MIMO) system is ideally suited for exploiting the spatial dimensions for interference mitigation [9]. The goal of this paper is to understand the fundamental limit of sparse recovery for mMTC. Specifically, we ask the following question. Given a pilot sequence length L and assuming a fixed set of non-orthogonal pilot sequences, how many (i.e., K) simultaneously active users can be identified out of a large number of N potential users, when the number of antennas M at the BS is large.

The answer to the above question depends on the way the problem is formulated. One possible formulation is the following. Because the wireless channels are time-varying and are not known precisely either at the transmitters or at the receiver, one can formulate the problem as a joint device activity detection and channel estimation problem. This approach is taken in [8], [9], where an approximate message-passing (AMP) algorithm is used for sparse recovery. For the case where the BS has a single antenna, we generally need $K < L$ for successful recovery. But interestingly, as pointed out in [9], as the number of BS antennas M goes to infinity, successful sparse recovery may be possible even for $K \geq L$, although AMP would become increasingly more difficult to converge at large M [10].

The above AMP approach falls under the Bayesian framework, as it assumes the knowledge of channel statistics and aims to estimate the instantaneous channel state information

This work was supported by the Natural Sciences and Engineering Research Council (NSERC) of Canada. The materials in this paper have been presented in part at the IEEE International Conference on Communications (ICC), Shanghai, China, May 2019 [1], and at the Asilomar Conference on Signals, Systems, and Computers, Pacific Grove, CA, USA, November 2019 [2].

Z. Chen, F. Sahrabi, and W. Yu are with The Edward S. Rogers Sr. Department of Electrical and Computer Engineering, University of Toronto, Toronto, ON M5S 3G4, Canada (e-mails: {zchen, fsahrabi, weiyu}@comm.utoronto.ca).

Y.-F. Liu is with the State Key Laboratory of Scientific and Engineering Computing, Institute of Computational Mathematics and Scientific/Engineering Computing, Academy of Mathematics and Systems Science, Chinese Academy of Sciences, Beijing, 100190, China (e-mail: yafliu@lsec.cc.ac.cn).

(CSI). An alternative formulation is to forgo the estimation of instantaneous CSI altogether, instead focusing on estimating the statistical channel information (in particular, the large-scale fading), and to use the estimated statistical information to determine whether a device is active or not. This non-Bayesian approach is pioneered in [11], and is termed the *covariance approach*, because a certain sample covariance matrix of the received sequence is a sufficient statistic for this estimation task. This covariance approach is ideally suited for large M , because the covariance can be accurately estimated using a large number of observation samples. When M is large, this covariance based approach has the key advantage that it is capable of detecting a much larger number of active devices, as observed in [10]–[12]. In fact, accurate activity detection is possible in the regime where $K = O(L^2)$.

The above scaling law is discovered in [10]–[12] for the asymptotic regime in which K , L , N , and M all go to infinity in certain way and is derived based on randomly generated pilot sequences so that the restricted isometry property of certain measurement matrix holds in the compressed sensing context [10]. In this paper, we revisit this issue and provide a more precise phase transition analysis for the covariance based approach from a completely different estimation theoretical perspective. Our analysis is non-asymptotic in the values of N , K , and L and works for arbitrary fixed pilot sequences under which reliable activity detection can be ensured in the large M limit. The investigation leads to a numerical method for characterizing the phase transition and an accurate prediction of the probability of detection error in the regime where M is large but finite.

It is pertinent to note that unlike the AMP approach, because the covariance approach does not reveal instantaneous CSI, to use the covariance approach for efficient data transmission, a subsequent channel estimation stage would normally be needed. However, if each device only has a small amount of data to transmit, it is possible to conceive a random access scheme in which each device is preassigned multiple distinct sequences, and the data bits are embedded in the choice of which sequence to transmit at each device, so that the BS can perform joint device activity and data detection [13]. The covariance approach is well suited for such a scenario, because of its $O(L^2)$ scaling that allows many more sequences to be detected. Our phase transition analysis of the covariance approach naturally carries over to this case.

A. Related Work

The classical random access strategy originated from the ALOHA system [14], which further evolved into a variety of enhanced ALOHA schemes [15]–[18] some of which employ iterative interference cancellation to resolve collision. The classical ALOHA can be thought of as a strategy that uses orthogonal sequences for device identification followed by collision resolution and retransmission.

Recently a number of non-orthogonal sequence based random access schemes for mMTC have been proposed, e.g., the two-phase grant-free random access [5], the grant-free random access with data embedding [13] or data spreading [19]. The

non-orthogonal sequences can be used as signatures for active device detection, e.g., [8], [11], [20], as codewords for data transmission, e.g., [12], [21], [22], or as both, e.g., [1], [13]. By detecting which sequences are transmitted, the BS acquires the identification of the active devices, or/and the data bits.

The sequence detection problem in random access is closely related to the compressed sensing problem due to the sporadic nature of the device activity, for which various sparse recovery techniques have been explored, e.g., orthogonal matching pursuit [23], [24], basis pursuit denoising [25], Bayesian sparse recovery [26], [27], and dimension reduction based optimization [28]. Specifically, the computationally efficient AMP algorithm is used for the device activity detection problem in [29]–[32] for single-antenna systems, in [8], [9], [33] for multi-antenna systems, and in [34], [35] for multi-cell or cloud radio access networks. An important feature of AMP is that the performance can be analyzed via an analytical framework of state evolution [36], based on which the detection error can be accurately predicted.

As mentioned earlier, when the BS is equipped with a large number of antennas, it is possible to detect the device activities by estimating the channel statistics based on certain sample covariance of the received signal. This covariance approach is proposed in [11], [12] for massive MIMO systems, where the sequence detection problem is formulated as either a maximum likelihood estimation (MLE) problem, or a nonnegative least square (NNLS) problem. The covariance based method is used in [11] for device activity detection and in [12] for data decoding. As compared to compressed sensing, the covariance based method exploits the channel hardening effect in the massive MIMO systems by averaging the received signal over antennas. It is shown in [11], [12] that when the number of BS antennas is large, the covariance based method with the MLE formulation can outperform AMP.

The performance of the covariance based approach under the NNLS formulation is recently analyzed in [10], where an error bound and an analytic scaling law on the system parameters are derived assuming a specific class of random pilot sequences. It is also shown in [10] that the same scaling law applies to a binary constrained version of the MLE formulation. In contrast to [10], this paper considers the generic MLE formulation with arbitrary sequences, and derives a necessary and sufficient condition for reliable activity detection for arbitrary finite K , L , and N . Our main result is a numerical characterization of phase transition.

Most of the above works that use non-orthogonal sequences as pilots take a *sourced* approach to massive connectivity. In contrast, an *unsourced* random access approach has been proposed in [21] and further developed in [12], [22], where the detection of device activities amounts to determining a list of messages from the active devices without identifying which message belongs to which device. The device identification information is embedded in the data payload. The detection problem for this scenario is different from the one considered here.

B. Main Contributions

This paper studies the covariance based approach for device activity detection with non-orthogonal sequences in a massive MIMO system. We adopt the MLE formulation and characterize the conditions for successful detection when the number of antennas at the BS tends to infinity. The main contributions are as follows:

- We study the performance of the device activity detection by analyzing the asymptotic behaviors of MLE via its associated Fisher information matrix. Given a device activity detection problem with finite N , K , and L , we derive a necessary and sufficient condition on the Fisher information matrix under which a vanishing detection error rate can be ensured as M tends to infinity. This condition involves solving a linear programming (LP) problem, based on which a numerical phase transition analysis can be obtained. As compared to the analytic scaling law derived in [10] that is asymptotic in N , K , L , and M , our phase transition analysis is numerical and asymptotic in M but non-asymptotic in N , K , and L . Moreover, the scaling law in [10] is based on a specific class of signature sequences that are uniformly drawn from a sphere, whereas our phase transition analysis applies to any arbitrary signature sequences.
- We provide an equivalent necessary and sufficient condition from the perspective of covariance matching to allow a characterization of the phase transition in N , K , and L , with M tending to infinity. The new condition reveals the connection between the phase transition analysis in this paper and the analytic scaling law in [10].
- We provide a way to accurately predict the error probabilities for device activity detection under finite M . This is accomplished by characterizing the distribution of the estimation error of MLE. We show that the distribution of detection error can be obtained by solving a quadratic programming (QP) problem involving the Fisher information matrix.
- Finally, we study the joint device activity and data detection for a random access scheme where each device is associated with multiple distinct sequences to convey a few data bits. We show that this joint device activity and data detection problem can be formulated in a similar way, and the performance can be analyzed accordingly.

C. Paper Organization and Notation

The remainder of this paper is organized as follows. Section II introduces the system model. Section III studies the device activity detection problem. Section IV analyzes the asymptotic performance and presents a phase transition analysis. Section V examines the phase transition analysis from the covariance matching perspective. Section VI studies the joint device activity and data detection problem. Simulation results are provided in Section VII. Conclusions are drawn in Section VIII.

Throughout this paper, lower-case, boldface lower-case, and boldface upper-case letters denote scalars, vectors, and

matrices, respectively. Calligraphy letters denote sets. Superscripts $(\cdot)^H$, $(\cdot)^T$, $(\cdot)^*$, $(\cdot)^{-1}$, and $(\cdot)^\dagger$ denote conjugate transpose, transpose, conjugate, inverse, and Moore-Penrose inverse, respectively. Further, \mathbf{I} denotes identity matrix with appropriate dimensions, $\mathbb{E}[\cdot]$ denotes expectation, $\text{Var}[\cdot]$ denotes variance, $\text{Re}(\cdot)$ denotes real part, $\text{Im}(\cdot)$ denotes imaginary part, $\text{tr}(\mathbf{X})$ denotes the trace of \mathbf{X} , $\text{diag}(x_1, \dots, x_n)$ (or $\text{diag}(\mathbf{X}_1, \dots, \mathbf{X}_n)$) denotes a (block) diagonal matrix formed by x_1, \dots, x_n (or $\mathbf{X}_1, \dots, \mathbf{X}_n$), \triangleq denotes definition, $|\cdot|$ denotes the determinant of a matrix, $\|\mathbf{X}\|_F$ denotes the Frobenius norm of \mathbf{X} , $\|\mathbf{x}\|_2$ denotes the ℓ_2 norm of \mathbf{x} , $\|\mathbf{x}\|_1$ denotes the ℓ_1 norm of \mathbf{x} , \odot denotes element-wise product, and \otimes denotes Kronecker product, $\mathcal{N}(\boldsymbol{\mu}, \boldsymbol{\Sigma})$ (or $\mathcal{CN}(\boldsymbol{\mu}, \boldsymbol{\Sigma})$) denotes a (complex) Gaussian distribution with mean $\boldsymbol{\mu}$ and covariance $\boldsymbol{\Sigma}$.

II. SYSTEM MODEL

Consider an uplink single-cell massive random access scenario with N single-antenna devices communicating with a BS equipped with M antennas. We primarily focus on the massive MIMO regime where M is large. A block fading channel model is assumed, i.e., the channel coefficients remain constant for a coherence interval. We assume that the user traffic is sporadic, i.e., only $K \ll N$ devices are active during each coherence interval. For the purpose of device identification, each device n is preassigned a unique signature sequence $\mathbf{s}_n = [s_{1n}, \dots, s_{Ln}]^T \in \mathbb{C}^L$, where L is the sequence length which is assumed to be shorter than the length of the coherence interval. In the pilot phase, we assume that all the active devices transmit their signature sequences synchronously at the same time. The objective is for the BS to detect which subset of devices are active based on the received signal.

Let $a_n \in \{1, 0\}$ denote the activity of device n in a given coherence interval, i.e., $a_n = 1$ if the device is active and $a_n = 0$ otherwise. We model the channel vector between the BS and device n as a random vector $g_n \mathbf{h}_n$, where $\mathbf{h}_n \in \mathbb{C}^M$ is the Rayleigh fading component that has the distribution $\mathcal{CN}(\mathbf{0}, \mathbf{I})$, and g_n is the large-scale fading component due to path-loss and shadowing. The received signal $\mathbf{Y} \in \mathbb{C}^{L \times M}$ at the BS in the pilot phase can be expressed as

$$\begin{aligned} \mathbf{Y} &= \sum_{n=1}^N a_n \mathbf{s}_n g_n \mathbf{h}_n^T + \mathbf{W} \\ &= [\mathbf{s}_1 \quad \dots \quad \mathbf{s}_N] \begin{bmatrix} a_1 g_1 & & \\ & \ddots & \\ & & a_N g_N \end{bmatrix} \begin{bmatrix} \mathbf{h}_1^T \\ \vdots \\ \mathbf{h}_N^T \end{bmatrix} + \mathbf{W} \\ &\triangleq \mathbf{S} \boldsymbol{\Gamma}^{\frac{1}{2}} \mathbf{H} + \mathbf{W}, \end{aligned} \quad (1)$$

where $\mathbf{S} \triangleq [\mathbf{s}_1, \dots, \mathbf{s}_N] \in \mathbb{C}^{L \times N}$ is the signature sequence matrix, $\boldsymbol{\Gamma} \triangleq \text{diag}\{\gamma_1, \dots, \gamma_N\} \in \mathbb{R}^{N \times N}$ with $\gamma_n = (a_n g_n)^2$ is a diagonal matrix indicating both the device activity a_n and the large-scale fading component g_n , $\mathbf{H} \triangleq [\mathbf{h}_1, \dots, \mathbf{h}_N]^T \in \mathbb{C}^{N \times M}$ is the channel matrix, and $\mathbf{W} \in \mathbb{C}^{L \times M}$ is the effective independent and identically distributed (i.i.d.) Gaussian noise with variance σ_w^2 normalized by the device transmit power for simplicity. We use $\boldsymbol{\gamma} \triangleq [\gamma_1, \dots, \gamma_N]^T \in \mathbb{R}^N$ to denote the diagonal entries of $\boldsymbol{\Gamma}$.

We assume that \mathbf{S} is known at the BS and exploit sparsity in identifying the device activity pattern (a_1, \dots, a_N) based on \mathbf{Y} . One way of formulating this detection problem is to estimate the instantaneous CSI $a_n g_n \mathbf{h}_n$ for all devices, as represented by the row sparse matrix $\mathbf{X} \triangleq \mathbf{\Gamma}^{\frac{1}{2}} \mathbf{H} \in \mathbb{C}^{N \times M}$. The active devices are simply devices with non-zero effective instantaneous channels. This is a compressed sensing problem of recovering non-zero rows of the matrix \mathbf{X} from the received signal $\mathbf{Y} = \mathbf{S}\mathbf{X} + \mathbf{W}$. If we assume prior knowledge or prior statistics of g_n , this problem can be solved under a Bayesian framework using, e.g., the AMP algorithm [8], [9].

An alternative formulation is to regard \mathbf{h}_n as random, and to detect the device activities by estimating only the $a_n g_n$ term for all devices. The active devices are simply ones whose effective large-scale fading coefficients are non-zero. This is akin to estimating the activity indicator a_n from the parameters of the channel statistics as represented by γ . In such a formulation, γ can be treated as a set of deterministic but unknown parameters, and \mathbf{Y} is modeled as an observation that follows the conditional distribution $p(\mathbf{Y}|\gamma)$ based on the statistics of \mathbf{h}_n and \mathbf{W} . This method is called *the covariance approach* [10]–[12], because of the essential role played by the sample covariance of \mathbf{Y} in the estimation process, as shown in the next section.

The key difference between the two approaches is that the estimation of γ involves a much smaller number of unknown parameters than the estimation of \mathbf{X} , so it is more efficient for detecting the device activities. On the other hand, the estimation of the channel statistics requires a large number of samples, so the covariance approach is most effective in the massive MIMO regime, where the large number of antennas provide many observation samples of the large-scale fading. When the number of BS antennas is small, the AMP-based approach may be preferable. This paper focuses attention to the massive MIMO regime. The aim is to provide a tractable performance analysis for the covariance based approach.

III. COVARIANCE BASED DEVICE ACTIVITY DETECTION

A. Problem Formulation

Following the approach suggested in [11], we use MLE to estimate γ from \mathbf{Y} , thereby obtaining the device activity indicator a_n . To compute the likelihood, we first observe from (1) that given γ , the columns of \mathbf{Y} , denoted by $\mathbf{y}_m \in \mathbb{C}^L$, $1 \leq m \leq M$, are independent due to the i.i.d. channel coefficients over the different antennas. Each column follows a complex Gaussian distribution as

$$\mathbf{y}_m \sim \mathcal{CN}(\mathbf{0}, \mathbf{S}\mathbf{\Gamma}\mathbf{S}^H + \sigma_w^2 \mathbf{I}), \quad (2)$$

where the covariance is obtained by computing $\mathbb{E}[\mathbf{y}_m \mathbf{y}_m^H]$ from (1). Let $\mathbf{\Sigma} \triangleq \mathbf{S}\mathbf{\Gamma}\mathbf{S}^H + \sigma_w^2 \mathbf{I}$. Due to the independence of the columns of \mathbf{Y} , the likelihood of \mathbf{Y} is

$$\begin{aligned} p(\mathbf{Y}|\gamma) &= \prod_{m=1}^M \frac{1}{|\pi \mathbf{\Sigma}|} \exp(-\mathbf{y}_m^H \mathbf{\Sigma}^{-1} \mathbf{y}_m) \\ &= \frac{1}{|\pi \mathbf{\Sigma}|^M} \exp(-\text{tr}(\mathbf{\Sigma}^{-1} \mathbf{Y}\mathbf{Y}^H)). \end{aligned} \quad (3)$$

The maximization of $\log p(\mathbf{Y}|\gamma)$ can be cast as the minimization of $-\frac{1}{M} \log p(\mathbf{Y}|\gamma)$ formulated as

$$\underset{\gamma}{\text{minimize}} \quad \log |\mathbf{\Sigma}| + \text{tr}(\mathbf{\Sigma}^{-1} \hat{\mathbf{\Sigma}}) \quad (4a)$$

$$\text{subject to} \quad \gamma \geq 0, \quad (4b)$$

where

$$\hat{\mathbf{\Sigma}} \triangleq \frac{1}{M} \mathbf{Y}\mathbf{Y}^H = \frac{1}{M} \sum_{m=1}^M \mathbf{y}_m \mathbf{y}_m^H \quad (5)$$

is the sample covariance matrix of the received signal averaged over different antennas, and $\gamma \geq 0$ is due to the fact that $\gamma_n = (a_n g_n)^2 \geq 0$, which defines a natural parameter space of γ .

We observe from (4) that the MLE problem depends on \mathbf{Y} through the sample covariance matrix $\hat{\mathbf{\Sigma}}$. For this reason, the approach based on solving the formulation in (4) is termed as the covariance based approach in this paper. As M increases, $\hat{\mathbf{\Sigma}}$ will tend to the true covariance matrix of \mathbf{Y} , but the size of the optimization problem does not change. Thus, the complexity of solving (4) does not scale with M , which is a desirable property especially in the massive MIMO regime.

It is worth mentioning that the use of maximum likelihood for parameter estimation with multivariate Gaussian observations has appeared in various contexts. For example, a similar optimization problem is formulated in [37] for the direction of arrival estimation. Other related examples include sparse approximation [38].

B. Algorithms

The optimization problem (4) is not convex in general due to the fact that $\log |\mathbf{\Sigma}|$ is concave whereas $\text{tr}(\mathbf{\Sigma}^{-1} \hat{\mathbf{\Sigma}})$ is convex. However, various algorithms have been shown to have excellent performance in practice for solving (4). For example, the authors of [38] propose a multiple sparse Bayesian learning (M-SBL) algorithm based on expectation maximization that estimates γ iteratively. The authors of [11] suggest a coordinate descent algorithm that randomly updates each coordinate of the estimate $\hat{\gamma}$ iteratively until convergence. Although the problem is non-convex, there is evidence that M-SBL or coordinate descent may be able to achieve global optimality if $\mathbf{\Gamma}^{\frac{1}{2}} \mathbf{H}$ or \mathbf{S} satisfies certain conditions; see [38] and [11].

For numerical experiments, this paper adopts the coordinate descent method from [11]. Once an estimate $\hat{\gamma}$ is obtained, we employ the element-wise thresholding to determine a_n from $\hat{\gamma}_i$, which is the i -th entry of $\hat{\gamma}$, with some threshold l_{th} , i.e., $a_n = 1$ if $\hat{\gamma}_i \geq l_{th}$ and $a_n = 0$ otherwise. The probabilities of missed detection and false alarm can be traded off by setting different values for l_{th} . A description of the coordinate descent algorithm is given in Algorithm 1. As compared to the algorithm in [11], we add random index permutation and rank-one update to further improve the efficiency. The complexity of the coordinate descent is dominated by the matrix-vector multiplications in steps 5–7, whose complexity is $\mathcal{O}(L^2)$. As a result, the overall complexity is $\mathcal{O}(TNL^2)$, where T is the number of iterations. Accordingly, as the complexity of the algorithm grows linearly in N and quadratically in L , it is

Algorithm 1 Coordinate descent to estimate γ

- 1: Initialize $\hat{\gamma} = \mathbf{0}$ and $\hat{\Sigma} = \sigma_w^2 \mathbf{I}$.
 - 2: **for** $i = 1, 2, \dots, T$ **do**
 - 3: Randomly select a permutation i_1, i_2, \dots, i_N of the coordinate indices $\{1, 2, \dots, N\}$ of $\hat{\gamma}$
 - 4: **for** $n = 1$ to N **do**
 - 5: $\delta = \max\left\{\frac{\mathbf{s}_{i_n}^H \hat{\Sigma}^{-1} \mathbf{Y} \mathbf{Y}^H \hat{\Sigma}^{-1} \mathbf{s}_{i_n} - \mathbf{s}_{i_n}^H \hat{\Sigma}^{-1} \mathbf{s}_{i_n}}{(\mathbf{s}_{i_n}^H \hat{\Sigma}^{-1} \mathbf{s}_{i_n})^2}, -\hat{\gamma}_{i_n}\right\}$
 - 6: $\hat{\gamma}_{i_n} \leftarrow \hat{\gamma}_{i_n} + \delta$
 - 7: $\hat{\Sigma}^{-1} \leftarrow \hat{\Sigma}^{-1} - \delta \frac{\hat{\Sigma}^{-1} \mathbf{s}_{i_n} \mathbf{s}_{i_n}^H \hat{\Sigma}^{-1}}{1 + \delta \mathbf{s}_{i_n}^H \hat{\Sigma}^{-1} \mathbf{s}_{i_n}}$
 - 8: **end for**
 - 9: **end for**
 - 10: Output $\hat{\gamma} = [\hat{\gamma}_1, \dots, \hat{\gamma}_N]^T$.
-

more suitable for scenarios with large N but small L , which is often the case for low-latency mMTC.

IV. ASYMPTOTIC PERFORMANCE ANALYSIS VIA FISHER INFORMATION MATRIX

It is challenging to analyze the performance of specific algorithms for solving the MLE problem (4), because most practical algorithms can only guarantee local optimality. In this section, we assume instead that the MLE problem (4) is solved to global optimality and analyze the asymptotic properties of the true MLE solution $\hat{\gamma}$ in the regime $M \rightarrow \infty$. Although the global minimizer of (4) may not be easily found in practice due to the computational complexity constraint, simulation results show that the analysis still provides useful insights into the performance of practical algorithms for solving (4). The analysis hinges upon the Fisher information matrix associated with the MLE problem.

For notational clarity, let γ^0 denote the true parameter to be estimated. We aim to study two questions: (i) What are the conditions on the system parameters N, K , and L such that the estimate $\hat{\gamma}$ can approach the true parameter γ^0 as $M \rightarrow \infty$? (ii) If these conditions are satisfied but if M is finite, how is the estimation error $\hat{\gamma} - \gamma^0$ distributed? The answer to the first question helps identify the desired operating regime in the space of N, K , and L for getting an accurate estimate $\hat{\gamma}$ via MLE with massive MIMO, and the answer to the second one helps characterize the error probabilities for practical device activity detection settings.

A. Asymptotic Properties of MLE

We investigate the above two questions by exploiting the asymptotic properties of MLE: *consistency* and *asymptotic normality*. Recall from (2) that the received signals \mathbf{y}_m at different antennas can be seen as i.i.d. samples of the underlying channel distribution. It is known from the standard estimation theory (e.g., [39]) that under certain regularity conditions, the MLE is *consistent*, i.e.,

$$\hat{\gamma} \xrightarrow{P} \gamma^0, \quad \text{as } M \rightarrow \infty, \quad (6)$$

where \xrightarrow{P} denotes convergence in probability. Furthermore, if the true parameter γ^0 is an interior point in the parameter

space of γ , the estimation error $\sqrt{M}(\hat{\gamma} - \gamma^0)$ converges in distribution to a multivariate Gaussian distribution as the number of i.i.d. samples goes to infinity, i.e.,

$$\sqrt{M}(\hat{\gamma} - \gamma^0) \xrightarrow{D} \mathcal{N}(0, M\mathbf{J}^{-1}(\gamma^0)), \quad \text{as } M \rightarrow \infty. \quad (7)$$

Here, $\mathbf{J}(\gamma)$ is the Fisher information matrix, whose (i, j) -th entry is defined as

$$[\mathbf{J}(\gamma)]_{ij} = \mathbb{E} \left[\left(\frac{\partial \log p(\mathbf{Y}|\gamma)}{\partial \gamma_i} \right) \left(\frac{\partial \log p(\mathbf{Y}|\gamma)}{\partial \gamma_j} \right) \right], \quad (8)$$

where $p(\mathbf{Y}|\gamma)$ is given in (3), and the expectation is taken with respect to \mathbf{Y} .

However, for the MLE problem considered in this paper, the results in (6) and (7) cannot be directly applied as two of the regularity conditions may not be satisfied:

- 1) The consistency of MLE requires that the true parameter γ^0 is *identifiable*, i.e., there exists no other $\gamma' \neq \gamma^0$ such that $p(\mathbf{Y}|\gamma') = p(\mathbf{Y}|\gamma^0)$. This may not be guaranteed in our problem because the dimension of the parameter γ^0 , i.e., N , could be much larger than the dimensions of the sample covariance matrix $\hat{\Sigma}$, i.e., $L \times L$, and therefore ambiguity may occur in the estimation of γ^0 .
- 2) The asymptotic normality of MLE requires that the true parameter γ^0 is an interior point of its parameter space, which is $[0, +\infty)^N$ in our problem, but γ^0 in fact lies on the boundary because most of the entries in γ^0 are zero. This boundary case makes the estimation error $\hat{\gamma} - \gamma^0$ always nonnegative at active coordinates, which leads to a non-Gaussian distribution for those coordinates.

In this paper, we deal with the issue of consistency by proposing a new necessary and sufficient condition for the parameter identifiability, and deal with the asymptotic distribution of $\sqrt{M}(\hat{\gamma} - \gamma^0)$ by taking the boundary case into consideration. Since the Fisher information matrix $\mathbf{J}(\gamma)$ plays a key role in our analysis, we first provide an explicit expression for $\mathbf{J}(\gamma)$.

Theorem 1: Consider the likelihood function in (3), where γ is the parameter to be estimated. The associated $N \times N$ Fisher information matrix of γ is given by

$$\mathbf{J}(\gamma) = M(\mathbf{P} \odot \mathbf{P}^*), \quad (9)$$

where $\mathbf{P} \triangleq \mathbf{S}^H (\mathbf{S}\mathbf{S}^H + \sigma_w^2 \mathbf{I})^{-1} \mathbf{S}$.

Proof: Please see Appendix A. ■

Note that it is possible that $\mathbf{J}(\gamma)$ is singular. This can be shown by using the fact that the rank of $\mathbf{J}(\gamma)$ must satisfy

$$\text{Rank}(\mathbf{P} \odot \mathbf{P}^*) \stackrel{(a)}{\leq} \text{Rank}(\mathbf{P})^2 \stackrel{(b)}{\leq} L^2, \quad (10)$$

where (a) is due to $\text{Rank}(\mathbf{U} \odot \mathbf{V}) \leq \text{Rank}(\mathbf{U}) \text{Rank}(\mathbf{V})$ for arbitrary matrices \mathbf{U} and \mathbf{V} , and (b) is based on $\text{Rank}(\mathbf{P}) \leq \min\{N, L\}$. Since $\mathbf{P} \odot \mathbf{P}^*$ is of size $N \times N$, we can conclude from (10) that $\mathbf{J}(\gamma)$ is singular if $N > L^2$, i.e., the dimension of γ is larger than the size of the sample covariance matrix $\hat{\Sigma}$ in (4). The singularity of $\mathbf{J}(\gamma)$ complicates the analysis of the estimation problem. Our analysis below takes singular $\mathbf{J}(\gamma)$ into consideration.

B. A Necessary and Sufficient Condition for Consistency of $\hat{\gamma}$

We first establish a necessary and sufficient condition on $\mathbf{J}(\gamma)$ such that $\hat{\gamma}$ can approach γ^0 in the large M limit.

Theorem 2: Consider the MLE problem in (4) for device activity detection with given signature sequence matrix $\mathbf{S} \in \mathbb{C}^{L \times N}$ and noise variance σ_w^2 , and let $\hat{\gamma}$ be the solution of (4). Let γ^0 be the true parameter whose $N - K$ zero entries are indexed by \mathcal{I} , i.e., $\mathcal{I} \triangleq \{i \mid \gamma_i^0 = 0\}$. Define

$$\mathcal{N} \triangleq \{\mathbf{x} \mid \mathbf{x}^T \mathbf{J}(\gamma^0) \mathbf{x} = 0, \mathbf{x} \in \mathbb{R}^N\}, \quad (11)$$

$$\mathcal{C} \triangleq \{\mathbf{x} \mid x_i \geq 0, i \in \mathcal{I}, \mathbf{x} \in \mathbb{R}^N\}, \quad (12)$$

where x_i is the i -th entry of \mathbf{x} . Then a necessary and sufficient condition for the consistency of $\hat{\gamma}$, i.e., $\hat{\gamma} \rightarrow \gamma^0$ as $M \rightarrow \infty$, is that the intersection of \mathcal{N} and \mathcal{C} is the zero vector, i.e., $\mathcal{N} \cap \mathcal{C} = \{\mathbf{0}\}$.

Proof: Please see Appendix B. ■

In Theorem 2, the set \mathcal{N} is the null space of $\mathbf{J}(\gamma^0)$ while the set \mathcal{C} is a cone with the coordinates indexed by \mathcal{I} being nonnegative. An interpretation of the condition $\mathcal{N} \cap \mathcal{C} = \{\mathbf{0}\}$ in Theorem 2 is as follows. The null space \mathcal{N} is a collection of all directions at γ^0 along which the log-likelihood function $\log p(\mathbf{Y}|\gamma)$ stays unchanged. This can be seen intuitively from (8). Based on (8), we have $\sum_i x_i \frac{\partial}{\partial \gamma_i} \log p(\mathbf{Y}|\gamma)|_{\gamma=\gamma^0} = 0$ whenever $\mathbf{x}^T \mathbf{J}(\gamma^0) \mathbf{x} = 0$ holds, implying that the directional derivative of $\log p(\mathbf{Y}|\gamma)$ at γ^0 along the direction \mathbf{x} is zero. On the other hand, the cone \mathcal{C} corresponds to all directions at γ^0 along which γ still remains in its feasible region, i.e., $[0, +\infty)^N$. It is because any point in both the neighborhood of γ^0 and in $[0, +\infty)^N$ can be expressed as $\gamma^0 + t\mathbf{x}$ for $\mathbf{x} \in \mathcal{C}$ and some positive scalar t . The condition $\mathcal{N} \cap \mathcal{C} = \{\mathbf{0}\}$ ensures that the likelihood function $p(\mathbf{Y}|\gamma)$ in the feasible neighborhood of γ^0 is not identical to that at γ^0 , i.e., $p(\mathbf{Y}|\gamma^0)$, and therefore the true parameter γ^0 is uniquely identifiable around its neighborhood through the likelihood function. Such a property is often referred to as the local identifiability [40], which is of course necessary to make $\hat{\gamma} \rightarrow \gamma^0$; otherwise, $\hat{\gamma}$ may converge to other neighboring points that have the identical likelihood function as $p(\mathbf{Y}|\gamma^0)$.

An example of \mathcal{N} and \mathcal{C} in \mathbb{R}^2 is illustrated in Fig. 1, where $\gamma^0 + \mathcal{C}$ indicates the feasible region (shaded) of γ around γ^0 , and \mathcal{N} represents a direction at γ^0 to the infeasible region of γ . Hence, the condition $\mathcal{N} \cap \mathcal{C} = \{\mathbf{0}\}$ is satisfied in Fig. 1.

Note that we use the notion of local identifiability of γ^0 to establish the necessity. To prove the sufficiency, we need to show that the true parameter γ^0 is also *globally* identifiable if $\mathcal{N} \cap \mathcal{C} = \{\mathbf{0}\}$ holds. For general estimation problems, it is usually difficult to examine the global identifiability based on its associated Fisher information matrix since the Fisher information matrix mainly provides local information on the likelihood function. However, the Gaussian model for the observations and the linearity (in γ) of the covariance matrix in the problem enable us to show that the local identifiability and the global identifiability are equivalent (see Appendix B). Due to this equivalence, the condition $\mathcal{N} \cap \mathcal{C} = \{\mathbf{0}\}$ is both necessary and sufficient. In the special case when $\mathbf{J}(\gamma^0)$ is non-singular (which is true with high probability if $N \leq L^2$ and

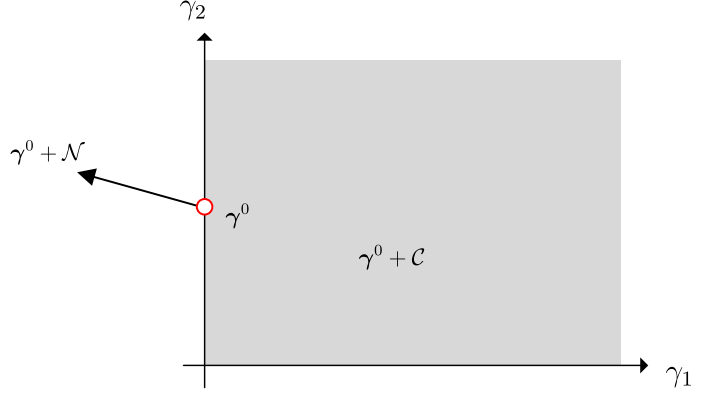


Fig. 1. An example of \mathcal{N} and \mathcal{C} in \mathbb{R}^2 . The shaded region represents the feasible set of γ , which is $[0, +\infty)^2$.

the entries of \mathbf{S} are generated randomly), we have $\mathcal{N} = \{\mathbf{0}\}$, and the condition in Theorem 2 is immediately satisfied.

Since there is no general closed-form characterization for $\mathcal{N} \cap \mathcal{C}$, the condition $\mathcal{N} \cap \mathcal{C} = \{\mathbf{0}\}$ for a given $\mathbf{J}(\gamma^0)$ cannot be verified analytically. However, by noting that the sets \mathcal{N} and \mathcal{C} are both convex, the condition can be numerically tested by searching for an N -dimensional non-zero vector in $\mathcal{N} \cap \mathcal{C}$. By further exploiting the positive semidefiniteness of the Fisher information matrix, the following theorem transforms the verification of $\mathcal{N} \cap \mathcal{C} = \{\mathbf{0}\}$ to an LP problem in a reduced $(N - K)$ -dimensional space.

Theorem 3: Given \mathbf{S} , σ_w^2 , and γ^0 , let $\mathbf{J}(\gamma^0)$ be the Fisher information matrix in (9). Let $\mathbf{A} \in \mathbb{R}^{(N-K) \times (N-K)}$ be a submatrix of $\mathbf{J}(\gamma^0)$ indexed by \mathcal{I} . Let $\mathbf{C} \in \mathbb{R}^{K \times K}$ be a submatrix of $\mathbf{J}(\gamma^0)$ indexed by \mathcal{I}^c , where \mathcal{I}^c is the complement of \mathcal{I} with respect to $\{1, 2, \dots, N\}$. Let $\mathbf{B} \in \mathbb{R}^{(N-K) \times K}$ be a submatrix of $\mathbf{J}(\gamma^0)$ with rows and columns indexed by \mathcal{I} and \mathcal{I}^c , respectively. Then the condition $\mathcal{N} \cap \mathcal{C} = \{\mathbf{0}\}$ in Theorem 2 is equivalent to: (i) \mathbf{C} is invertible; and (ii) the following problem is feasible

$$\text{find } \mathbf{x} \quad (13a)$$

$$\text{subject to } (\mathbf{A} - \mathbf{B}\mathbf{C}^{-1}\mathbf{B}^T)\mathbf{x} > \mathbf{0}, \quad (13b)$$

where vector $\mathbf{x} \in \mathbb{R}^{N-K}$.

Proof: Please see Appendix C. ■

Theorem 3 shows that if there exists a vector \mathbf{x} in \mathbb{R}^{N-K} such that $(\mathbf{A} - \mathbf{B}\mathbf{C}^{-1}\mathbf{B}^T)\mathbf{x}$ lies in the positive orthant, then $\mathcal{N} \cap \mathcal{C} = \{\mathbf{0}\}$ holds. Note that the feasibility problem in (13) depends only on the matrix $\mathbf{A} - \mathbf{B}\mathbf{C}^{-1}\mathbf{B}^T$. The class of such matrices that satisfy the constraint in (13b) is referred to as \mathcal{M}^+ , which is introduced in [41] in the study of the NNLS problem, and also used in [10] for the performance analysis of device activity detection via the NNLS formulation. It is interesting that, while we formulate the estimation of γ^0 as an MLE problem instead of an NNLS problem, the notion of \mathcal{M}^+ still appears.

The condition derived in Theorem 2 can be efficiently tested numerically by solving (13) for fixed problem parameters. Since $\mathbf{A} - \mathbf{B}\mathbf{C}^{-1}\mathbf{B}^T$ is determined by $\mathbf{J}(\gamma^0)$, which depends on \mathbf{S} , σ_w^2 , and γ^0 , the solution to (13) could also potentially depend on all of these parameters. However, we show later in

Section V-A that the solution actually only depends on \mathbf{S} and the index set \mathcal{I} corresponding to γ^0 . Suppose that \mathbf{S} and \mathcal{I} are generated randomly for any fixed N , L , and K (e.g., \mathbf{S} is Gaussian and the elements in \mathcal{I} are uniformly selected from $\{1, 2, \dots, N\}$), we can use (13) to test different realizations of \mathbf{S} and \mathcal{I} . This gives us a way of numerically identifying the phase transition of this problem, i.e., the region in the space of N , L , and K such that $\hat{\gamma}$ can approach γ^0 in the large M limit.

C. Distribution of Estimation Error $\hat{\gamma} - \gamma^0$

We now assume that the system parameters are in the operating regime where the estimator $\hat{\gamma}$ is consistent, i.e., it converges to the true γ^0 as $M \rightarrow \infty$, and aim to characterize the distribution of the estimation error $\hat{\gamma} - \gamma^0$ for finite M . We achieve this by characterizing the asymptotic distribution of $\sqrt{M}(\hat{\gamma} - \gamma^0)$. As mentioned before, $\sqrt{M}(\hat{\gamma} - \gamma^0)$ does not tend to a Gaussian distribution, since γ^0 lies on the boundary of its feasible space. The following theorem considers the fact that γ^0 is a boundary point, and characterizes the asymptotic distribution of $\sqrt{M}(\hat{\gamma} - \gamma^0)$ via a QP problem.

Theorem 4: Consider the maximum likelihood estimator $\hat{\gamma}$ of the device activity detection problem with given \mathbf{S} , σ_w^2 , at finite M . Let γ^0 be the true activity pattern. Let $\mathbf{J}(\gamma^0)$ be the Fisher information matrix defined in (9). Let \mathcal{N} and \mathcal{C} be defined as in (11) and (12), respectively. Assume that $\mathcal{N} \cap \mathcal{C} = \{\mathbf{0}\}$. Let $\mathbf{x} \in \mathbb{R}^N$ be a random vector sampled from $\mathcal{N}(\mathbf{0}, M\mathbf{J}^\dagger(\gamma^0))$. For each \mathbf{x} , let $\boldsymbol{\mu} \in \mathbb{R}^N$ be the solution to the following constrained QP

$$\underset{\boldsymbol{\mu}}{\text{minimize}} \quad \frac{1}{M}(\mathbf{x} - \boldsymbol{\mu})^T \mathbf{J}(\gamma^0)(\mathbf{x} - \boldsymbol{\mu}) \quad (14a)$$

$$\text{subject to} \quad \boldsymbol{\mu} \in \mathcal{C}. \quad (14b)$$

Then, $\sqrt{M}(\hat{\gamma} - \gamma^0)$ has asymptotically the same distribution as $\boldsymbol{\mu}$ as $M \rightarrow \infty$.

Proof: Please see Appendix D. ■

Note that $\boldsymbol{\mu}$ is random due to the randomness of \mathbf{x} . The idea here is to draw a sample \mathbf{x} from the Gaussian distribution specified by the Fisher information matrix, then to project the sample to the cone \mathcal{C} so that the estimation error is consistent with the fact that the true γ^0 lies on the boundary.

Based on Theorem 4, the distribution of the estimation error $\hat{\gamma} - \gamma^0$ for finite M can be approximated by that of $\boldsymbol{\mu}/\sqrt{M}$. Since QP does not admit a closed-form solution in general, it is difficult to obtain the distribution of the estimation error analytically. However, Theorem 4 is still useful in the sense that it reveals the connection between the Fisher information matrix and the error distribution, and it also enables us to numerically obtain the error distribution by solving (14).

V. PHASE TRANSITION ANALYSIS FROM A COVARIANCE MATCHING PERSPECTIVE

The necessary and sufficient condition in Theorem 2 is based on the properties of the maximum likelihood estimation and its associated Fisher information matrix. In this section, we provide an equivalent condition from a perspective of

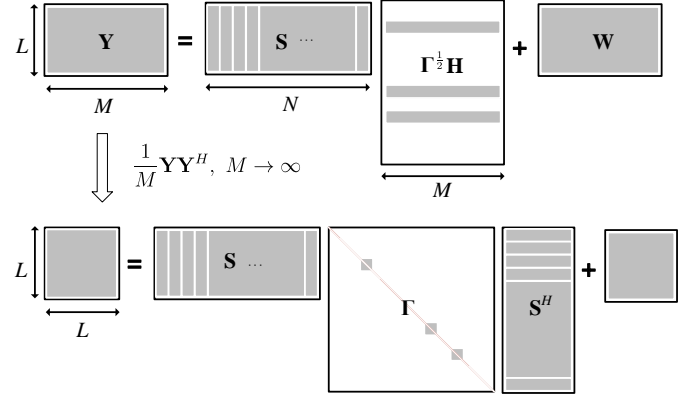


Fig. 2. A visualization of the covariance matching as $M \rightarrow \infty$.

covariance matching by directly analyzing the optimization problem in (4). This new perspective provides new insight into the phase transition analysis, and also shows the connection to a recent analytic scaling law derived in [10].

A. Covariance Matching as $M \rightarrow \infty$

First, let us consider a relaxed version of (4), where the optimization is performed over Σ instead of γ . A closed-form solution can be obtained immediately as $\Sigma = \hat{\Sigma}$ by checking the optimality condition of the objective $\log |\Sigma| + \text{tr}(\Sigma^{-1}\hat{\Sigma})$. Unfortunately, under finite M , the closed-form solution $\Sigma = \hat{\Sigma}$ may not lead to a feasible solution for γ due to the fact that the sample covariance matrix may not exhibit the structure that the true covariance matrix should have, i.e., it may not be possible to express $\hat{\Sigma} = \frac{1}{M}\mathbf{Y}\mathbf{Y}^H$ as $\mathbf{S}\mathbf{\Gamma}\mathbf{S}^H + \sigma_w^2\mathbf{I}$ for some nonnegative diagonal matrix $\mathbf{\Gamma}$. Therefore, the solution for γ cannot be easily obtained from $\hat{\Sigma}$. However, in the asymptotic regime $M \rightarrow \infty$ where the sample covariance matrix $\hat{\Sigma}$ converges to the true covariance matrix, $\mathbf{S}\mathbf{\Gamma}^0\mathbf{S}^H + \sigma_w^2\mathbf{I}$ where $\mathbf{\Gamma}^0 \triangleq \text{diag}(\gamma_1^0, \dots, \gamma_N^0)$, it is guaranteed that a feasible solution for γ exists, which can be found by solving for $\mathbf{\Gamma}$ in

$$\mathbf{S}\mathbf{\Gamma}\mathbf{S}^H + \sigma_w^2\mathbf{I} = \hat{\Sigma} \quad (15)$$

under the constraint that $\mathbf{\Gamma}$ is a diagonal matrix with nonnegative entries. The equation (15) in the limit $M \rightarrow \infty$ can be seen as the matching of the sample covariance matrix and the true covariance matrix, which is visualized in Fig. 2.

Since the true parameter γ^0 , or equivalently $\mathbf{\Gamma}^0$, must be a solution to (15), intuitively, to make $\hat{\gamma} \rightarrow \gamma^0$ as $M \rightarrow \infty$, we need to make sure that γ^0 is the unique solution to (15) in the regime $M \rightarrow \infty$ under the nonnegative constraint. This is accomplished by analyzing the null space of the vectorized form of (15) as below:

$$\widehat{\mathbf{S}}(\gamma - \gamma^0) = \mathbf{0}, \quad (16)$$

where $\widehat{\mathbf{S}} \in \mathbb{C}^{L^2 \times N}$ is the column-wise Kronecker product (Khatri-Rao product) of \mathbf{S}^* and \mathbf{S} written as

$$\widehat{\mathbf{S}} = [\mathbf{s}_1^* \otimes \mathbf{s}_1, \mathbf{s}_2^* \otimes \mathbf{s}_2, \dots, \mathbf{s}_N^* \otimes \mathbf{s}_N]. \quad (17)$$

A necessary and sufficient condition to guarantee that the true parameter γ^0 is the unique solution to (16) under the nonnegative constraint in the limit $M \rightarrow \infty$ is stated as follows:

Theorem 5: Consider the covariance matching problem (15) with $\hat{\Sigma}$ as defined by (5) with the true value of the activity pattern being γ^0 . For the given signature sequence matrix \mathbf{S} , let $\hat{\mathbf{S}} \in \mathbb{C}^{L^2 \times N}$ be the column-wise Kronecker product of \mathbf{S}^* and \mathbf{S} given in (17). We define set $\tilde{\mathcal{N}}$ in \mathbb{R}^N as

$$\tilde{\mathcal{N}} \triangleq \{\mathbf{x} \mid \hat{\mathbf{S}}\mathbf{x} = \mathbf{0}, \mathbf{x} \in \mathbb{R}^N\}. \quad (18)$$

Then a necessary and sufficient condition for $\mathbf{\Gamma}^0 = \text{diag}\{\gamma^0\}$ to be the unique nonnegative solution to (15) in the limit $M \rightarrow \infty$ is $\tilde{\mathcal{N}} \cap \mathcal{C} = \{\mathbf{0}\}$, where \mathcal{C} is defined in (12).

Proof: Please see Appendix E. ■

The following result reveals the equivalence between the consistency of $\hat{\gamma}$ and the uniqueness of the nonnegative solution to (15) in the regime $M \rightarrow \infty$, by showing that the condition $\mathcal{N} \cap \mathcal{C} = \{\mathbf{0}\}$ in Theorem 2 and $\tilde{\mathcal{N}} \cap \mathcal{C} = \{\mathbf{0}\}$ in Theorem 5 are actually equivalent.

Theorem 6: The sets $\tilde{\mathcal{N}}$ defined in (18) and \mathcal{N} defined in (11) are identical, hence the condition $\tilde{\mathcal{N}} \cap \mathcal{C} = \{\mathbf{0}\}$ is equivalent to $\mathcal{N} \cap \mathcal{C} = \{\mathbf{0}\}$.

Proof: Please see Appendix F. ■

Note that \mathcal{N} in (11) is defined as the null space of $\mathbf{J}(\gamma^0)$, which is determined by \mathbf{S} , σ_w^2 , and γ^0 as shown in (9), whereas $\tilde{\mathcal{N}}$ in (18) is defined as the null space of $\hat{\mathbf{S}}$, which depends only on \mathbf{S} . The equivalence between $\tilde{\mathcal{N}}$ and \mathcal{N} indicates that σ_w^2 and γ^0 , although involved in the expression of $\mathbf{J}(\gamma^0)$, have no impact on the null space of $\mathbf{J}(\gamma^0)$. By further noticing that \mathcal{C} is determined by \mathcal{I} , we can conclude that the satisfiability of $\mathcal{N} \cap \mathcal{C} = \{\mathbf{0}\}$ in Theorem 2 only depends on \mathbf{S} and the support of γ^0 ; it does not depend on σ_w^2 or the values of the non-zero entries of γ^0 . This gives us a way of numerically analyzing the phase transition of both the MLE and the matrix matching approaches, as a function of only K , L , and N , in the massive MIMO regime.

Similar to Theorem 3, we can examine whether $\tilde{\mathcal{N}} \cap \mathcal{C} = \{\mathbf{0}\}$ holds for given $\hat{\mathbf{S}}$ and \mathcal{I} by solving an LP problem. Since $\hat{\mathbf{S}}$ is complex while $\tilde{\mathcal{N}}$ is a real subspace, we need to separate the real and imaginary parts of $\hat{\mathbf{S}}$. Let $\mathbf{r}_i^T = [s_{i1}, s_{i2}, \dots, s_{iN}]$ be the i -th row of \mathbf{S} . Based on \mathbf{r}_i^T , we construct two sets of row vectors to represent the real and imaginary parts of rows of $\hat{\mathbf{S}}$:

$$\{\text{Re}(\mathbf{r}_i^T) \odot \text{Re}(\mathbf{r}_j^T) + \text{Im}(\mathbf{r}_i^T) \odot \text{Im}(\mathbf{r}_j^T), 1 \leq i \leq j \leq L\} \quad (19)$$

and

$$\{\text{Re}(\mathbf{r}_i^T) \odot \text{Im}(\mathbf{r}_j^T) - \text{Im}(\mathbf{r}_i^T) \odot \text{Re}(\mathbf{r}_j^T), 1 \leq i < j \leq L\}. \quad (20)$$

In total, these two sets consist of L^2 vectors in $\mathbb{R}^{1 \times N}$. Let $\mathbf{D} \in \mathbb{R}^{L^2 \times N}$ be the matrix formed by all L^2 row vectors from the two sets.

Theorem 7: The condition $\tilde{\mathcal{N}} \cap \mathcal{C} = \{\mathbf{0}\}$ is equivalent to the infeasibility of the following problem

$$\text{find } \mathbf{x} \quad (21a)$$

$$\text{subject to } \mathbf{D}\mathbf{x} = \mathbf{0}, \quad (21b)$$

$$\mathbf{1}^T \mathbf{x} = 1, \quad (21c)$$

$$x_i \geq 0, i \in \mathcal{I}, \quad (21d)$$

where $\mathbf{x} \in \mathbb{R}^N$ and the constraint (21c) guarantees $\mathbf{x} \neq \mathbf{0}$.

Proof: Please see Appendix G. ■

As compared to the LP in (13), the LP in (21) does not include the true parameter γ^0 and the noise variance σ_w^2 ; the solution to (21) depends on \mathbf{S} and \mathcal{I} only. There is also a slight difference in dimensionality. The LP in (13) aims to find an $(N - K)$ -dimensional vector under $N - K$ inequality constraints, whereas the LP in (21) aims to find an N -dimensional vector under $L^2 + 1$ equality constraints and $N - K$ inequality constraints.

B. Connection to the Scaling Law in [10]

The condition $\tilde{\mathcal{N}} \cap \mathcal{C} = \{\mathbf{0}\}$ derived in this paper provides a precise criterion for any given \mathbf{S} and \mathcal{I} under any setups of N , L , and K to ensure reliable activity detection as M tends to infinity. The satisfiability of $\tilde{\mathcal{N}} \cap \mathcal{C} = \{\mathbf{0}\}$ can be tested numerically for any finite N , L , and K .

A recent work in [10] studies a similar problem but focuses on the NNLS formulation, and derives an analytic scaling law on N , L , K , and M for a specific class of signature sequences that are drawn uniformly from a sphere in \mathbb{C}^L , such that the device activity can be reliably detected. Specifically, it is shown in [10] that the number of identifiable active devices is $K = O(L^2)$, up to a logarithmic factor and a universal constant for sufficiently large M , using the covariance based NNLS formulation, which aims to solve the following problem

$$\underset{\gamma}{\text{minimize}} \quad \|\Sigma - \hat{\Sigma}\|_F^2 \quad (22a)$$

$$\text{subject to } \gamma \geq 0. \quad (22b)$$

Note that in the asymptotic regime $M \rightarrow \infty$ with fixed N , K , and L , NNLS becomes the covariance matching problem discussed in Section V-A. Therefore, the results in Section V-A should be related to the scaling law in [10]. To show the connection, we use the following results derived in [10, Theorem 2, Theorem 4], based on which the scaling law in [10] is established.

Lemma 1 ([10]): Let $\mathbf{S} \in \mathbb{C}^{L \times N}$ be the signature sequence matrix whose columns are uniformly drawn from the sphere of radius \sqrt{L} in an i.i.d. fashion. There exist some constants c_1 , c_2 , c_3 , and c_4 whose values do not depend on K , L , and N such that if $K \leq c_1 L^2 / \log^2(eN/L^2)$, then with probability at least $1 - \exp(-c_2 L)$, the following two statements are true:

- 1) The matrix $\hat{\mathbf{S}}$ defined in (17) has the ℓ_2 robust null space property (NSP) of order K with parameters $0 < \rho < 1$ and $\tau > 0$. More precisely, the following inequality

$$\|\mathbf{x}_{\mathcal{K}}\|_2 \leq \frac{\rho}{\sqrt{K}} \|\mathbf{x}_{\mathcal{K}^c}\|_1 + \tau \|\hat{\mathbf{S}}\mathbf{x}\|_2 \quad (23)$$

holds for any $\mathbf{x} \in \mathbb{R}^N$ and any index set $\mathcal{K} \subseteq \{1, 2, \dots, N\}$ with $|\mathcal{K}| \leq K$, where $\mathbf{x}_{\mathcal{K}}$ is a sub-vector of \mathbf{x} with entries from \mathcal{K} , and \mathcal{K}^c is the complementary set of \mathcal{K} with respect to $\{1, 2, \dots, N\}$.

2) The solution of (22), $\hat{\gamma}^{\text{NNLS}}$, satisfies

$$\|\gamma^0 - \hat{\gamma}^{\text{NNLS}}\|_2 \leq c_3 \left(\sqrt{\frac{L}{K}} + c_4 \right) \frac{\|\Sigma^0 - \hat{\Sigma}\|_F}{L}, \quad (24)$$

where $\Sigma^0 = \mathbf{S}\Gamma^0\mathbf{S}^H + \sigma_w^2\mathbf{I}$.

Proof: Please see [10]. ■

Assuming $M \rightarrow \infty$, (24) implies that the estimation error in NNLS vanishes when N , K , and L are large due to the fact that the sample covariance matrix converges to the true covariance matrix. Based on Lemma 1, the following theorem shows that $\tilde{\mathcal{N}} \cap \mathcal{C} = \{\mathbf{0}\}$ can also be ensured under the conditions in Lemma 1.

Theorem 8: Under the same scaling law for K , L , N and for the same randomly chosen \mathbf{S} as specified in Lemma 1, $\tilde{\mathcal{N}} \cap \mathcal{C} = \{\mathbf{0}\}$ in Theorem 5 holds with probability at least $1 - \exp(-c_2L)$.

Proof: Please see Appendix H. ■

Based on Theorem 8 and the equivalence between \mathcal{N} and $\tilde{\mathcal{N}}$, we can conclude that once the system parameters satisfy the scaling law, the condition $\mathcal{N} \cap \mathcal{C} = \{\mathbf{0}\}$ also holds with high probability. Therefore, with sufficiently large M , the activity pattern of the devices can be reliably detected by solving the MLE problem. Theorem 8 shows that the scaling law derived for the NNLS formulation also applies to the MLE formulation. Note that in practice, MLE achieves a substantially lower error probability as compared to NNLS at finite M , as shown in the simulations in Section VII.

C. Regularization

It is worth mentioning that in both the MLE formulation and the NNLS formulation, γ is treated as a set of deterministic but unknown parameters. This means that the fact that the true parameter γ^0 is a sparse vector is not exploited. A straightforward way of incorporating such prior information is to add a regularization term to the objective functions in (4) and (22) to promote the sparsity of the solution. For example, we can consider l_1 regularizer, i.e., $R(\gamma) = \lambda \sum_{n=1}^N \gamma_n$, or log-sum regularizer, i.e., $R(\gamma) = \lambda \sum_{n=1}^N \log(\epsilon + \gamma_n)$ with $\epsilon > 0$, where λ is a tunable parameter. With the regularization term, the new objective, based on (4), becomes

$$\min_{\gamma \geq 0} \log |\Sigma| + \text{tr} \left(\Sigma^{-1} \hat{\Sigma} \right) + \frac{1}{M} R(\gamma). \quad (25)$$

However, such a regularization term may not be necessary. This can be justified by the identifiability of γ^0 in the MLE formulation or the uniqueness of γ^0 to the NNLS problem in the limit $M \rightarrow \infty$, provided that the condition $\tilde{\mathcal{N}} \cap \mathcal{C} = \{\mathbf{0}\}$ is satisfied. Similar arguments have been discussed in [41] and [10] for NNLS. Moreover, it is generally not easy to choose the parameter λ properly. In the simulation part of this paper, we evaluate the impact of the regularization under finite M . The results show that, although the regularization cannot help

improve the detection performance substantially as expected, it changes the trade-off between the two types of errors in the device activity detection.

VI. JOINT DEVICE ACTIVITY AND DATA DETECTION

This section aims to show that the above analysis can also be applied to the scenario in which each device is associated with multiple signature sequences and can embed a few information bits in the random access phase. We aim to show that the joint device activity and data detection problem can be formulated as an optimization problem similar to (4) via MLE, and an asymptotic performance analysis can be carried out using the approach discussed in Sections IV and V.

Suppose that each active device has b bits to send. To encode the b -bit data as well as the device identification, we assume that each device is assigned a unique set of $Q \triangleq 2^b$ sequences with length L , which can be represented by a matrix as $\mathbf{S}_n = [\mathbf{s}_n^1, \mathbf{s}_n^2, \dots, \mathbf{s}_n^Q] \in \mathbb{C}^{L \times Q}$, where $\mathbf{s}_n^q \in \mathbb{C}^L$ is the q -th sequence of device n . Each active device selects one sequence to transmit. Let $a_n^q \in \{1, 0\}$ indicate whether or not sequence q of device n is transmitted. We have that $\sum_{q=1}^Q a_n^q \in \{0, 1\}$ for each n , where $\sum_{q=1}^Q a_n^q = 0$ implies that device n is inactive. Similar to (1), the received signal at the BS is given by

$$\tilde{\mathbf{Y}} = \sum_{n=1}^N \mathbf{S}_n \mathbf{D}_n \mathbf{H}_n + \tilde{\mathbf{W}} \triangleq \tilde{\mathbf{S}} \tilde{\Gamma}^{\frac{1}{2}} \tilde{\mathbf{H}} + \tilde{\mathbf{W}}, \quad (26)$$

where $\mathbf{D}_n \triangleq \text{diag}\{a_n^1 g_n, \dots, a_n^Q g_n\} \in \mathbb{R}^{Q \times Q}$ is a diagonal matrix showing the sequence selection and the large-scale fading of device n , $\mathbf{H}_n \triangleq [\mathbf{h}_n, \dots, \mathbf{h}_n]^T \in \mathbb{C}^{Q \times M}$ is the channel matrix formed by repeated rows, $\tilde{\mathbf{W}} \in \mathbb{C}^{L \times M}$ is the effective i.i.d. Gaussian noise with variance σ_w^2 , $\tilde{\mathbf{S}} \triangleq [\mathbf{S}_1, \dots, \mathbf{S}_N] \in \mathbb{C}^{L \times NQ}$, $\tilde{\Gamma}^{\frac{1}{2}} \triangleq \text{diag}\{\mathbf{D}_1, \dots, \mathbf{D}_N\} \in \mathbb{R}^{NQ \times NQ}$, and $\tilde{\mathbf{H}} \triangleq [\mathbf{H}_1^T, \dots, \mathbf{H}_N^T]^T \in \mathbb{C}^{NQ \times M}$. Note that (26) differs from (1) in the extra block structure exhibited in $\tilde{\Gamma}$ and $\tilde{\mathbf{H}}$.

The BS performs the joint device activity and data detection by estimating the diagonal matrix $\tilde{\Gamma}$ based on $\tilde{\mathbf{Y}}$. Note that the columns of $\tilde{\mathbf{Y}}$ can be seen as independent samples drawn from a complex Gaussian distribution with mean zero and covariance $\tilde{\Sigma}$, which can be computed from (26) as

$$\tilde{\Sigma} = \mathbb{E}[\tilde{\mathbf{Y}}\tilde{\mathbf{Y}}^H] = \tilde{\mathbf{S}} \tilde{\Gamma}^{\frac{1}{2}} \Phi \tilde{\Gamma}^{\frac{1}{2}} \tilde{\mathbf{S}}^H + \sigma_w^2 \mathbf{I}, \quad (27)$$

where $\Phi \triangleq \text{diag}\{\mathbf{E}, \dots, \mathbf{E}\} \in \mathbb{R}^{NQ \times NQ}$ is a block diagonal matrix with $\mathbf{E} \in \mathbb{R}^{Q \times Q}$ being the all-one matrix. Since each diagonal block \mathbf{D}_n in $\tilde{\Gamma}^{\frac{1}{2}}$ has at most one non-zero entry, the covariance matrix can be simplified as $\tilde{\Sigma} = \tilde{\mathbf{S}} \tilde{\Gamma} \tilde{\mathbf{S}}^H + \sigma_w^2 \mathbf{I}$.

Let $\tilde{\gamma} \in \mathbb{R}^{NQ}$ be the diagonal entries of $\tilde{\Gamma}$, i.e., $\tilde{\gamma} = [\tilde{\gamma}_1^T, \dots, \tilde{\gamma}_N^T]^T$ with $\tilde{\gamma}_n = [(a_n^1 g_n)^2, \dots, (a_n^Q g_n)^2]^T \in \mathbb{R}^Q$. We use MLE to estimate $\tilde{\gamma}$. The maximization of $\log p(\tilde{\mathbf{Y}}|\tilde{\gamma})$ can be cast as the following optimization problem

$$\underset{\tilde{\gamma}}{\text{minimize}} \quad \log |\tilde{\Sigma}| + \frac{1}{M} \text{tr} \left(\tilde{\Sigma}^{-1} \tilde{\mathbf{Y}} \tilde{\mathbf{Y}}^H \right) \quad (28a)$$

$$\text{subject to} \quad \tilde{\gamma} \geq 0, \quad (28b)$$

$$|\tilde{\gamma}_n|_0 \leq 1, \quad n = 1, 2, \dots, N, \quad (28c)$$

where $|\cdot|_0$ denotes the number of non-zero entries of a vector, and (28c) comes from the sequence selection of each active device, i.e., $\sum_{q=1}^Q a_n^q \in \{0, 1\}$.

As compared to (4), the extra blockwise constraint (28c) makes problem (28) difficult to solve. In this paper, we consider a heuristic method to deal with (28) by first dropping constraint (28c). The rationale is that, based on the analysis in Theorem 2, if the Fisher information matrix associated with $\tilde{\gamma}$ satisfies the condition in Theorem 2, it is guaranteed that the resulting estimate of $\tilde{\gamma}$ without considering (28c) converges to its true value as $M \rightarrow \infty$, indicating that (28c) is satisfied automatically due to the consistency. For large but finite M , since (28c) may not be satisfied exactly, we then use a simple coordinate selection to enforce the constraint for each block.

Using such a method implies that the results in Theorem 2 as well as Theorem 5 and Theorem 6 can be used to obtain a phase transition analysis on $N2^b$, K , and L . Moreover, the result in Theorem 4 can be used to characterize the error probability in the joint device activity and data detection.

VII. SIMULATION RESULTS

In this section, we validate the asymptotic results via simulations, and demonstrate the detection performance of the covariance based method for the random access. We consider an mMTC system with one cell of radius 1000m, where all devices are located at the cell-edge for simplicity. Note that this scenario also corresponds to the case when all devices are distributed randomly in the cell but with a power control scheme in which the transmit power of each device is inversely proportional to its large-scale fading. The power of the background noise is considered to be -169dBm/Hz over 10 MHz, and the transmit power of each device is set as 23dBm . We assume that all sequences are generated from an i.i.d. complex Gaussian distribution with zero mean and unit variance, unless otherwise specified.

A. Numerical Validation of the Phase Transition

We consider the device activity detection problem, and numerically test the sufficient and necessary condition described in Theorem 2 under a variety of choices of L and K , given $N = 1000$ or $N = 4000$. We draw the region of L, K in which the condition is satisfied. Note that the satisfiability of the condition does not depend on σ_w^2 , as shown in Theorem 7, and thus we fix σ_w^2 in the simulations. We are interested in the case $L^2 < N$ such that the Fisher information matrix $\mathbf{J}(\gamma^0)$ is singular. Otherwise, the non-singular Fisher information matrix already guarantees that the condition is satisfied. Further, since the detection of K active devices is based on effective $O(L^2)$ observations of the covariance matrix, we plot L^2/N versus K/N in Fig. 3. Given L and K , we generate $\mathbf{J}(\gamma^0)$ based on random \mathbf{S} and γ^0 , and identify the region where the condition can/cannot be satisfied. The result is obtained based on 100 realizations of \mathbf{S} and γ^0 for each K and L . The error bars indicate the range beyond which either all 100 realizations or zero realization satisfy the condition. Note that the error bar is due to the randomness of \mathbf{S} and γ^0 . To validate the prediction from Theorem 2, we also run the coordinate descent algorithm to solve the MLE problem in (4) in the large M limit, i.e., with ideal sample covariance matrix, to empirically plot a phase transition curve.

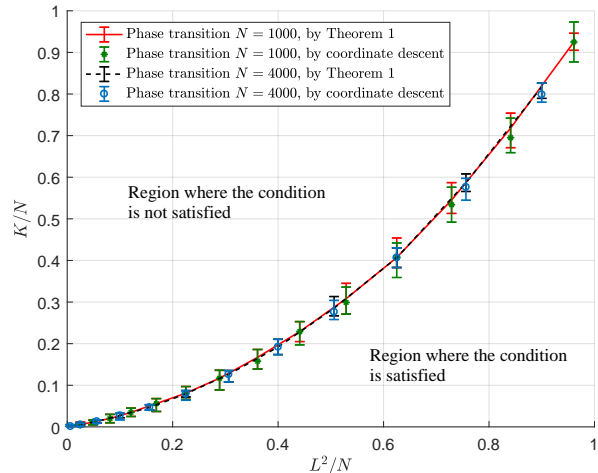


Fig. 3. Phase transition of the covariance based method for device activity detection.

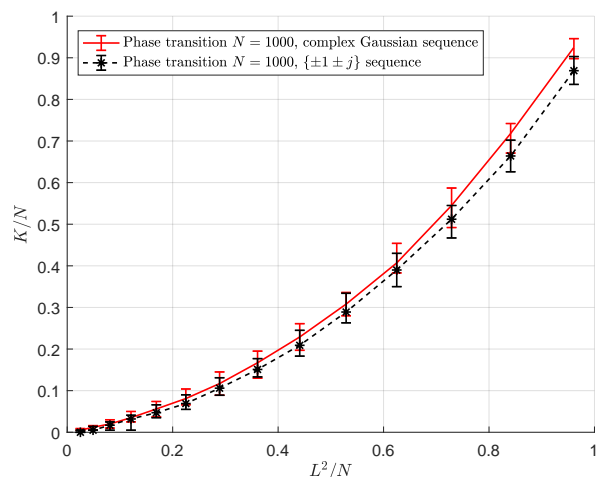


Fig. 4. Phase transition comparison of the complex Gaussian signature sequences and the signature sequences whose entries are from $\{\pm 1 \pm j\}$.

We observe from Fig. 3 that the curves with different values of N overlap, and the transition region becomes narrower with larger N , implying that the phase transition depends on N, L , and K via the ratios L^2/N and K/N . We also observe that the curves obtained by Theorem 2 and obtained by the coordinate descent match well.

Since the condition in Theorem 2 is applicable to any arbitrary sequence matrix \mathbf{S} , we can use the condition to evaluate the phase transitions for different types of signature sequence matrices. Fig. 4 compares the complex Gaussian matrix with another random matrix whose elements are uniformly drawn from a finite alphabet, $\{\pm 1 \pm j\}$. We observe from Fig. 4 that the Gaussian matrix slightly outperforms the matrix generated from $\{\pm 1 \pm j\}$. But from a practical point of view, it is easier to generate and store the sequence matrix with $\{\pm 1 \pm j\}$.

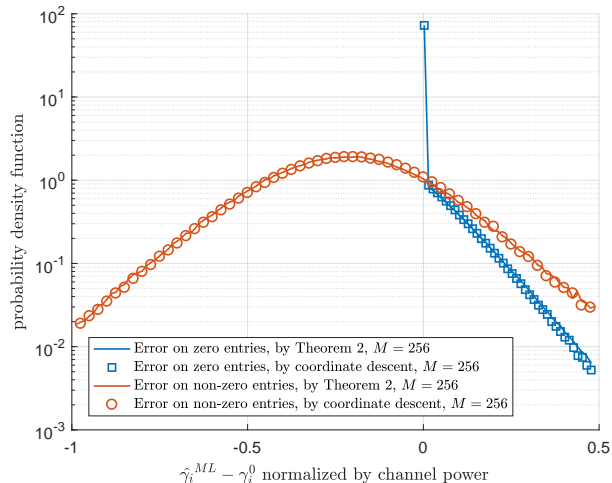


Fig. 5. Probability density functions (PDFs) of the error on the zero entries and on the non-zero entries.

B. Distribution of the Estimation Error

In Fig. 5, we validate the approximated distribution of $\hat{\gamma} - \gamma^0$ with $M = 256$ from Theorem 4, by comparing it with the result from running the coordinate descent algorithm to solve (4). We set $N = 1000$, $K = 50$, and $L = 20$, which corresponds to $L^2/N = 0.4$ and $K/N = 0.05$ in Fig. 3. We treat each coordinate of $\hat{\gamma} - \gamma^0$ as independent for simplicity to plot the empirical distribution of the coordinate-wise error. We consider two types of coordinates depending on whether or not the true value on that coordinate is zero, and plot their corresponding distributions separately. We observe that the curves by Theorem 4 match those by solving (4) with coordinate descent in both cases. We observe that there is a point mass in the distribution of the error for the zero entries. This is the probability that the inactive devices are correctly identified at finite $M = 256$.

The distribution of the estimation error in Fig. 5 helps characterize the probabilities of missed detection and false alarm for the device activity detection problem. A trade-off between missed detection and false alarm can be obtained by setting different thresholds in the last step of the activity detection. We compare the predicted result by the error distribution in Theorem 4 and the simulated result by the coordinate descent algorithm in Fig. 6 with $N = 1000$, $K = 50$, and $L = 20$. We observe that the simulated and theoretical curves match very well. The gap becomes even smaller when the number of antennas increases.

C. Joint Device Activity and Data Detection

In this subsection, we validate the phase transition analysis and the characterization of the estimation error in MLE for joint device activity and data detection. The phase transition is shown in Fig. 7, where $N = 1000$ and b is set as 1 or 2. We plot $K/(N2^b)$ versus $L^2/(N2^b)$, i.e., both K/N and L^2/N are normalized by an extra factor 2^b . We observe from Fig. 7 that the curves obtained by Theorem 2 and obtained by the coordinate descent match well. Moreover, we also observe

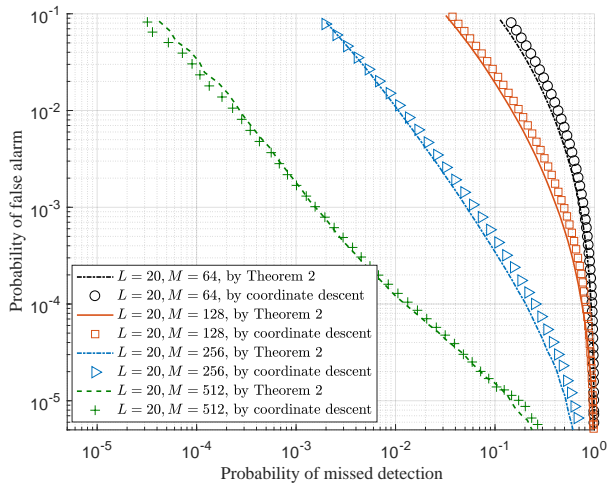


Fig. 6. Comparison of the simulated results and the analysis in terms of probability of false alarm and probability of missed detection for device activity detection.

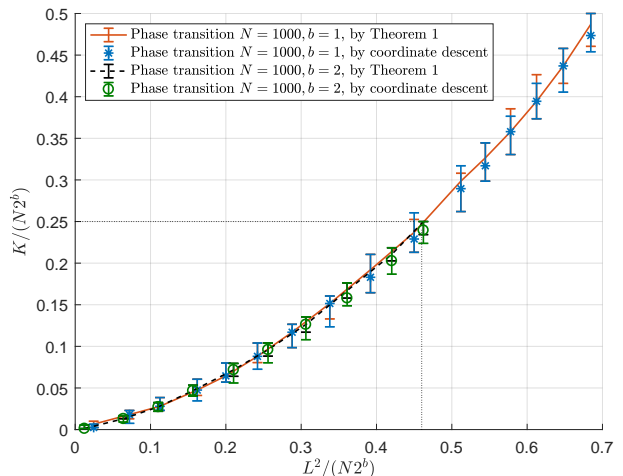


Fig. 7. Phase transition of the covariance based method for joint device activity and data detection.

that the curves with $b = 1$ and $b = 2$ are partially overlapped, indicating that the phase transition depends on N , L , K , and b via the ratios $L^2/(N2^b)$ and $K/(N2^b)$.

Similar to Fig. 6, the characterization of the estimation error in MLE can be used to predict the performance of joint device activity and data detection. Here, we still use the probability of false alarm and the probability of missed detection as the performance metrics. To take both device activity and data detection into consideration, we slightly modify the definitions of these two types of errors. Specifically, the probability of missed detection corresponds to two types of error events: a device is active but is declared to be inactive, or a device is active but the data is not correctly decoded although the device is declared active. The probability of false alarm corresponds to the event that a device is inactive but declared active no matter what the decoded data is. A trade-off between missed detection and false alarm can be obtained by setting different

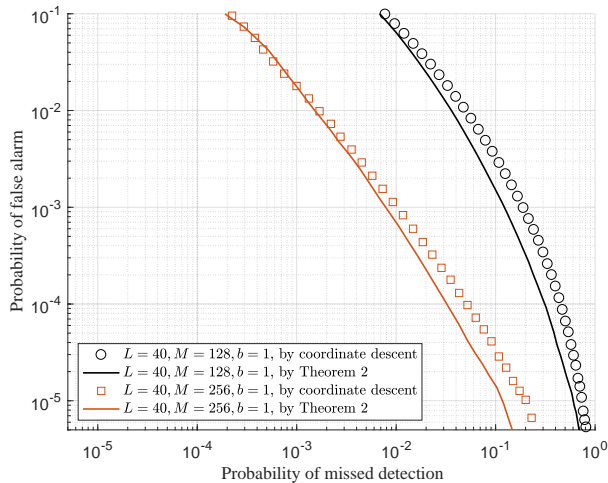


Fig. 8. Comparison of the simulated results and the analysis in terms of probability of false alarm and probability of missed detection for joint device activity and data detection .

thresholds. Fig. 8 shows the predicted and the simulated trade-off curves with $N = 1000$, $K = 100$, $b = 1$, and $L = 40$. As compared to Fig. 6, the prediction becomes slightly less accurate, which might be due to the extra block-wise sparsity in $\tilde{\gamma}$ because of information embedding.

D. MLE vs. NNLS vs. AMP

In this subsection, we consider the joint device activity and data detection problem, and compare the covariance based method with the AMP based method that has been used to solve a similar problem for massive random access in [13]. For the covariance based method, we consider both the MLE formulation employed in this paper and the NNLS formulation studied in [10]. We fix $N = 1000$, $K = 100$, and consider various values for L and M . We set $b = 1$ or $b = 2$, i.e., each active device has 1 or 2 bits of information to transmit.

In Fig. 9, we show the detection performance as the signature sequence length L increases. Since there are two types of detection errors, to conveniently show the error behavior with L , we properly select the threshold to achieve a point where the probability of false alarm and the probability of missed detection are equal, which is represented as “probability of error” in Fig. 9. We observe that increasing L substantially decreases the error probability for the covariance based method with the MLE formulation. However, for the AMP based method, the benefit of increasing L becomes obvious only when L exceeds some point, e.g., $L = 80$ when $b = 2$. This can be explained by the phase transition in AMP [36], which requires L to be sufficiently large, depending on the problem size. We also observe from Fig. 9 that the covariance based method with the MLE formulation consistently outperforms both the AMP based method and the covariance based method with the NNLS formulation. Moreover, by increasing the transmitted data from 1 bit to 2 bits, which doubles the size of the set of the non-orthogonal sequences, AMP suffers from far more severe performance degradation as compared to the covariance based methods.

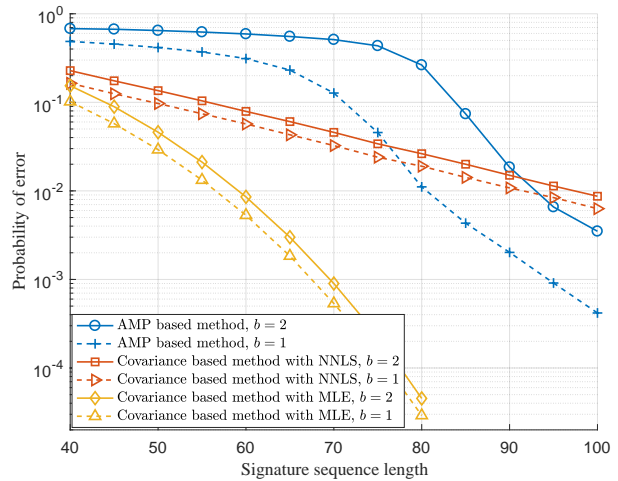


Fig. 9. Performance comparison of the covariance based method with MLE, the covariance based method with NNLS, and the AMP based method under different L , where $M = 64$.

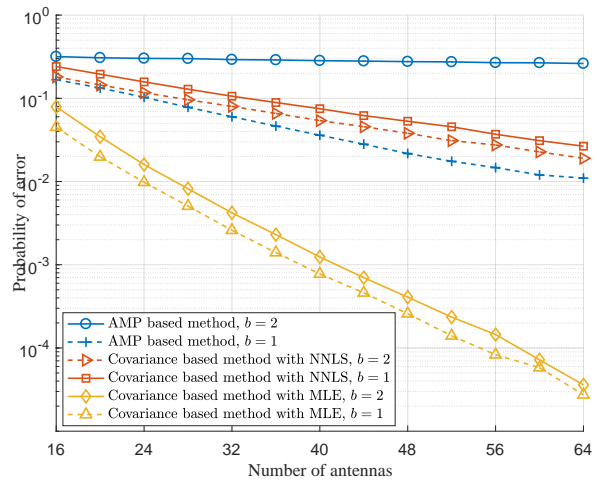


Fig. 10. Performance comparison of the covariance based method with MLE, the covariance based method with NNLS, and the AMP based method under different M , where $L = 80$.

In Fig. 10, we compare the covariance based methods and the AMP based method as the number of antennas at the BS increases. We consider the signature length $L = 80$, and show the behavior of the detection error as a function of M . We observe that for the covariance based method with the MLE formulation the error drops effectively as M increases, whereas for the AMP based method, the error becomes saturated when M exceeds some point, e.g., $M = 56$ when $b = 1$. This can be explained by the state evolution of AMP in [9] which requires that L grows faster than M to fully exploit the benefit of multiple antennas. We also observe from Fig. 10 that the detection error drops at a much higher rate in the MLE formulation as compared to the NNLS formulation.

Fig. 9 and Fig. 10 show that MLE substantially outperforms the AMP based method when M is large and $L < K$, which is the preferable operating regime of the covariance

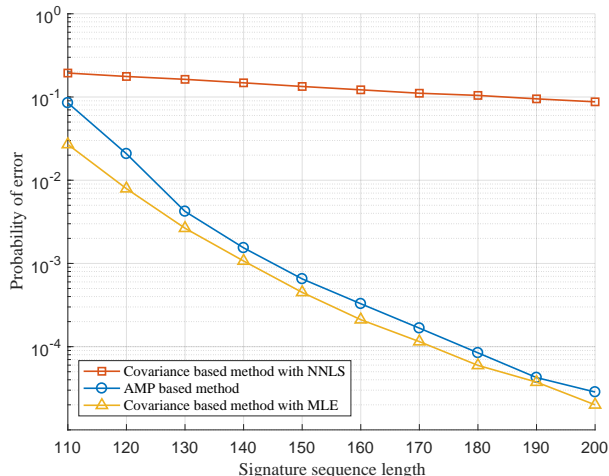


Fig. 11. Performance comparison of the covariance based method with MLE, the covariance based method with NNLS, and the AMP based method under different L , where $M = 8$ and $b = 1$.

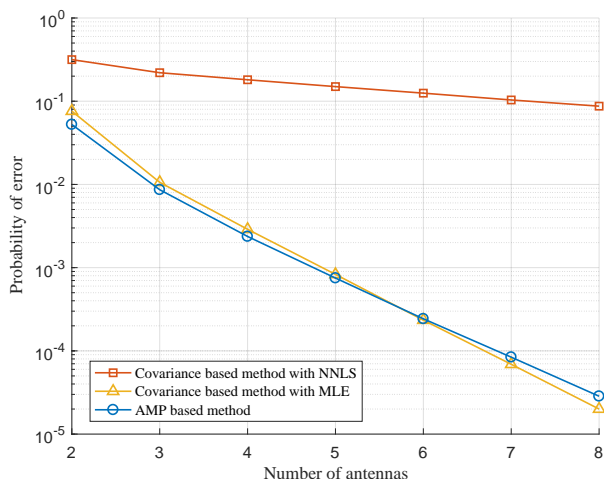


Fig. 12. Performance comparison of the covariance based method with MLE, the covariance based method with NNLS, and the AMP based method under different M , where $L = 200$ and $b = 1$.

based method. However, it is worth mentioning that in the scenario where M is small and L is relatively large as compared to K , these two methods can achieve comparable performance, as illustrated in Fig. 11 and Fig. 12. In such a case, the AMP based method has the advantage of lower computational complexity, which is largely attributed to the fact that the complexity in AMP scales with L linearly per iteration whereas Algorithm 1 for solving the MLE problem scales with L quadratically per iteration. For small M and $L > K$, a comparison of the overall computational time of those two methods implemented in Matlab on a computer with Intel Core i5-5200U CPU and 8 GB of memory is shown in Fig. 13, from which we observe that the AMP based method indeed has lower complexity and better scalability with L .

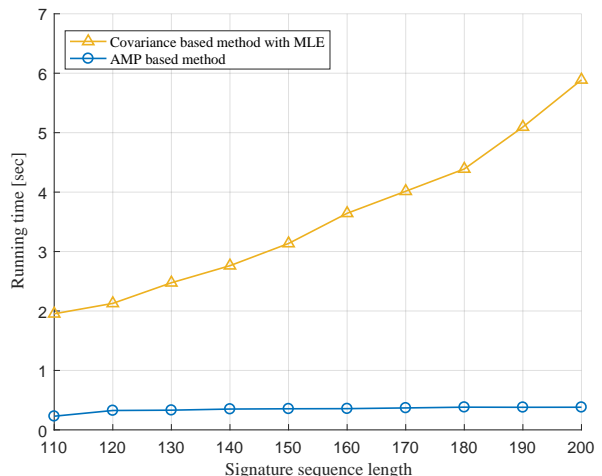


Fig. 13. Computational time comparison of the covariance based method with MLE and the AMP based method under different L , where $M = 8$ and $b = 1$.

E. Impact of Regularization

In the last part of the simulations, we investigate the impact of adding a regularization term to the objective in (4) under finite M . We consider two different regularization terms, l_1 regularizer and log-sum regularizer, discussed in Section V-B. We consider the device activity detection problem for a system with $N = 1000$, $K = 50$, $L = 30$, and $M = 64$. We use the coordinate descent algorithm to solve (25). Similar to Algorithm 1, closed-form expressions can be derived for the coordinate updates. In Fig. 14, we plot the probability of missed detection versus the probability of false alarm under different choices of λ . We observe that the regularization terms, especially the log-sum regularizer, change the trade-off between the two types of detection errors. Specifically, for the log-sum regularizer, we observe that when the probability of missed detection is set to be larger than 0.02 (or 0.05) for $\lambda = 1$ (or $\lambda = 4$), the regularization term leads to smaller probability of false alarm. In the meanwhile, with the log-sum regularizer it becomes harder to achieve a very low probability of missed detection, no matter what the probability of false alarm is. The change in the trade-off can be explained by the fact that the regularization term indeed promotes the sparsity of the solution, which makes the occurrence of the false alarm more unlikely; but it also increases the chance of missing one or two active devices among all active devices.

VIII. CONCLUSION

This paper studies the device activity detection problem for the random access that relies on the use of the non-orthogonal sequences in mMTC with massive MIMO. A covariance based approach is employed which formulates the activity detection problem as an MLE problem. By analyzing the asymptotic behaviors of MLE via its associated Fisher information matrix, a necessary and sufficient condition on the Fisher information matrix, under which a vanishing detection error is guaranteed in the massive MIMO regime, is derived. This leads to a

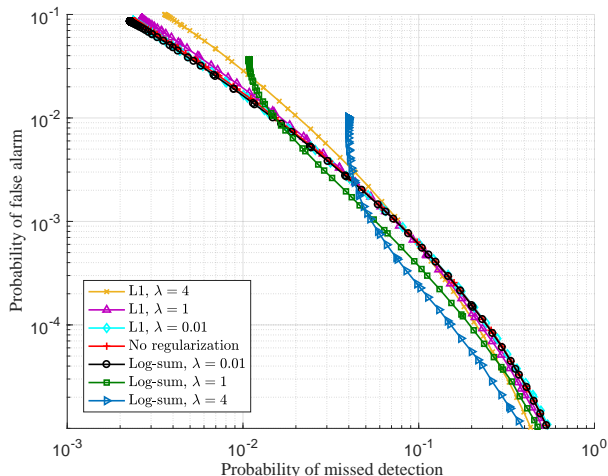


Fig. 14. Probabilities of false alarm and missed detection with the regularization term in the log-likelihood function.

phase transition analysis based on solving an LP that divides the space of the system parameters into success and failure regions. When the condition is satisfied, this paper further provides an approach based on solving a QP to accurately predict the probabilities of detection error for device activity detection with a finite number of antennas. This paper also considers a random access scheme consisting of joint device activity and data detection, and shows that the joint detection problem can be formulated in a similar way to the device activity detection problem and admits a similar performance analysis.

APPENDIX

A. Proof of Theorem 1

We compute the (i, j) -th entry of the Fisher information matrix by using the following identity [39, Eq. (3.23)]

$$\mathbb{E} \left[\frac{\partial \log p(\mathbf{Y}|\boldsymbol{\gamma})}{\partial \gamma_i} \frac{\partial \log p(\mathbf{Y}|\boldsymbol{\gamma})}{\partial \gamma_j} \right] = -\mathbb{E} \left[\frac{\partial^2 \log p(\mathbf{Y}|\boldsymbol{\gamma})}{\partial \gamma_i \partial \gamma_j} \right], \quad (29)$$

because it is easier to obtain an explicit expression from the right-hand side of (29) for the problem under consideration. Let $\mathcal{L}(\boldsymbol{\gamma}) \triangleq \log p(\mathbf{Y}|\boldsymbol{\gamma})$. The first-order derivative of $\mathcal{L}(\boldsymbol{\gamma})$ is given by

$$\frac{\partial \mathcal{L}(\boldsymbol{\gamma})}{\partial \gamma_i} = -M \operatorname{tr} \left(\boldsymbol{\Sigma}^{-1} \mathbf{s}_i \mathbf{s}_i^H \right) + M \operatorname{tr} \left(\boldsymbol{\Sigma}^{-1} \mathbf{s}_i \mathbf{s}_i^H \boldsymbol{\Sigma}^{-1} \hat{\boldsymbol{\Sigma}} \right), \quad (30)$$

and its second-order partial derivative can be computed as

$$\begin{aligned} \frac{\partial^2 \mathcal{L}(\boldsymbol{\gamma})}{\partial \gamma_i \partial \gamma_j} &= M \operatorname{tr} \left(\boldsymbol{\Sigma}^{-1} \mathbf{s}_j \mathbf{s}_j^H \boldsymbol{\Sigma}^{-1} \mathbf{s}_i \mathbf{s}_i^H \right) \\ &\quad - M \operatorname{tr} \left(\boldsymbol{\Sigma}^{-1} \mathbf{s}_j \mathbf{s}_j^H \boldsymbol{\Sigma}^{-1} \mathbf{s}_i \mathbf{s}_i^H \boldsymbol{\Sigma}^{-1} \hat{\boldsymbol{\Sigma}} \right) \\ &\quad - M \operatorname{tr} \left(\boldsymbol{\Sigma}^{-1} \mathbf{s}_i \mathbf{s}_i^H \boldsymbol{\Sigma}^{-1} \mathbf{s}_j \mathbf{s}_j^H \boldsymbol{\Sigma}^{-1} \hat{\boldsymbol{\Sigma}} \right). \end{aligned} \quad (31)$$

By taking the expectation with respect to \mathbf{Y} using $\mathbb{E}[\hat{\boldsymbol{\Sigma}}] = \boldsymbol{\Sigma}$, we get the (i, j) -th entry of the Fisher information matrix as

$$\begin{aligned} -\mathbb{E} \left[\frac{\partial^2 \mathcal{L}(\boldsymbol{\gamma})}{\partial \gamma_i \partial \gamma_j} \right] &= M \operatorname{tr} \left(\boldsymbol{\Sigma}^{-1} \mathbf{s}_i \mathbf{s}_i^H \boldsymbol{\Sigma}^{-1} \mathbf{s}_j \mathbf{s}_j^H \right) \\ &= M \left(\mathbf{s}_i^H \boldsymbol{\Sigma}^{-1} \mathbf{s}_j \right) \left(\mathbf{s}_j^H \boldsymbol{\Sigma}^{-1} \mathbf{s}_i \right), \end{aligned} \quad (32)$$

based on which $\mathbf{J}(\boldsymbol{\gamma})$ can be written in a matrix form as (9).

B. Proof of Theorem 2

We use the notion of identifiability in MLE, i.e., the true parameter $\boldsymbol{\gamma}^0$ is (globally) identifiable if there exists no other $\boldsymbol{\gamma}' \neq \boldsymbol{\gamma}^0$ such that $p(\mathbf{Y}|\boldsymbol{\gamma}') = p(\mathbf{Y}|\boldsymbol{\gamma}^0)$. For the problem under consideration, it can be shown that the consistency of $\hat{\boldsymbol{\gamma}}$ holds if and only if the true parameter is identifiable based on the result in [42, Theorem 14.1]. Therefore, in this proof we aim to show that $\mathcal{N} \cap \mathcal{C} = \{\mathbf{0}\}$ is necessary and sufficient for the identifiability of $\boldsymbol{\gamma}^0$.

We start by introducing the notion of *local* identifiability [40]. As compared to the (global) identifiability, the local identifiability of $\boldsymbol{\gamma}^0$ only requires that there exists a neighborhood of $\boldsymbol{\gamma}^0$ such that it contains no other $\boldsymbol{\gamma}' \neq \boldsymbol{\gamma}^0$ with $p(\mathbf{Y}|\boldsymbol{\gamma}') = p(\mathbf{Y}|\boldsymbol{\gamma}^0)$. We first prove that $\mathcal{N} \cap \mathcal{C} = \{\mathbf{0}\}$ is necessary and sufficient for the local identifiability of $\boldsymbol{\gamma}^0$. We then show that the local identifiability is equivalent to the global identifiability for the problem under consideration, which completes the proof.

First, we present two lemmas on the null space of $\mathbf{J}(\boldsymbol{\gamma})$.

Lemma 2: Let $\boldsymbol{\Sigma} = \mathbf{U}\boldsymbol{\Lambda}\mathbf{U}^H$ be the eigenvalue decomposition of the covariance matrix $\boldsymbol{\Sigma} = \boldsymbol{\Sigma}\boldsymbol{\Gamma}\boldsymbol{\Sigma}^H + \sigma_w^2\mathbf{I}$ with $\boldsymbol{\gamma} \geq \mathbf{0}$. Let $\mathbf{V} \triangleq \mathbf{S}^H\mathbf{U} \in \mathbb{C}^{N \times L}$, and denote its i -th column by \mathbf{v}_i . Then the set of $\mathbf{x} \in \mathbb{R}^N$ satisfying $\mathbf{x}^T \mathbf{J}(\boldsymbol{\gamma}) \mathbf{x} = 0$ is given by

$$\{\mathbf{x} \mid \mathbf{x}^T (\mathbf{v}_i \odot \mathbf{v}_j^*) = 0, \forall 1 \leq i, j \leq L\}. \quad (33)$$

Proof: Let the eigenvalues of $\boldsymbol{\Sigma}$ be $\boldsymbol{\Lambda} = \operatorname{diag}\{\lambda_1, \lambda_2, \dots, \lambda_L\}$. By plugging $\boldsymbol{\Sigma} = \mathbf{U}\boldsymbol{\Lambda}\mathbf{U}^H$ into (9), $\mathbf{J}(\boldsymbol{\gamma})$ can be expressed as

$$\begin{aligned} \mathbf{J}(\boldsymbol{\gamma}) &= (\mathbf{S}^H \mathbf{U} \boldsymbol{\Lambda}^{-1} \mathbf{U}^H \mathbf{S}) \odot (\mathbf{S}^H \mathbf{U} \boldsymbol{\Lambda}^{-1} \mathbf{U}^H \mathbf{S})^* \\ &= (\mathbf{V} \boldsymbol{\Lambda}^{-1} \mathbf{V}^H) \odot (\mathbf{V} \boldsymbol{\Lambda}^{-1} \mathbf{V}^H)^* \\ &= \left(\sum_{i=1}^L \lambda_i^{-1} \mathbf{v}_i \mathbf{v}_i^H \right) \odot \left(\sum_{j=1}^L \lambda_j^{-1} \mathbf{v}_j^* \mathbf{v}_j^T \right) \\ &= \sum_{i=1}^L \sum_{j=1}^L (\lambda_i^{-1} \mathbf{v}_i \mathbf{v}_i^H) \odot (\lambda_j^{-1} \mathbf{v}_j^* \mathbf{v}_j^T) \\ &= \sum_{i=1}^L \sum_{j=1}^L \lambda_i^{-1} \lambda_j^{-1} (\mathbf{v}_i \odot \mathbf{v}_j^*) (\mathbf{v}_i \odot \mathbf{v}_j^*)^H, \end{aligned} \quad (34)$$

where the last step is due to the fact that $(\mathbf{v}_i \mathbf{v}_i^H) \odot (\mathbf{v}_j^* \mathbf{v}_j^T) = (\mathbf{v}_i \odot \mathbf{v}_j^*) (\mathbf{v}_i^H \odot \mathbf{v}_j^T)$. Note that $\boldsymbol{\Sigma}$ is positive definite when $\boldsymbol{\gamma} \geq \mathbf{0}$, which implies that λ_i 's are all positive. Moreover, $(\mathbf{v}_i \odot (\mathbf{v}_j^*)) (\mathbf{v}_i \odot (\mathbf{v}_j^*))^H, 1 \leq i, j \leq L$, are all positive semidefinite. Therefore, any $\mathbf{x} \in \mathbb{R}^N$ satisfying $\mathbf{x}^T \mathbf{J}(\boldsymbol{\gamma}^0) \mathbf{x} = 0$ must also satisfy

$$\mathbf{x}^T (\mathbf{v}_i \odot \mathbf{v}_j^*) = 0, \forall 1 \leq i, j \leq L, \quad (35)$$

and vice versa, from which we obtain (33). ■

Lemma 3: If \mathbf{x} is such that $\mathbf{x}^T \mathbf{J}(\gamma^0) \mathbf{x} = 0$, then $\mathbf{x}^T \mathbf{J}(\gamma) \mathbf{x} = 0$ also holds for any $\gamma \geq 0$.

Proof: The variables \mathbf{U} , $\mathbf{\Lambda}$, \mathbf{V} , and \mathbf{v}_i in Lemma 2 all depend on γ . Let \mathbf{U}_0 , $\mathbf{\Lambda}_0$, \mathbf{V}_0 , and \mathbf{v}_i^0 be the values of \mathbf{U} , $\mathbf{\Lambda}$, \mathbf{V} , and \mathbf{v}_i , corresponding to γ^0 . Since $\mathbf{V} \triangleq \mathbf{S}^H \mathbf{U}$ and $\mathbf{V}_0 \triangleq \mathbf{S}^H \mathbf{U}_0$, we have

$$\mathbf{V} = \mathbf{V}_0 \mathbf{U}_0^H \mathbf{U} = \mathbf{V}_0 \bar{\mathbf{U}}, \quad (36)$$

where $\bar{\mathbf{U}} \triangleq \mathbf{U}_0^H \mathbf{U}$. Let the (i, j) -th entry of $\bar{\mathbf{U}}$ be \bar{u}_{ij} . By writing (36) explicitly as $\mathbf{v}_i = \sum_{l=1}^L \bar{u}_{li} \mathbf{v}_l^0$, we get

$$\begin{aligned} \mathbf{v}_i \odot \mathbf{v}_j^* &= \left(\sum_{l=1}^L \bar{u}_{li} \mathbf{v}_l^0 \right) \odot \left(\sum_{k=1}^L \bar{u}_{kj}^* (\mathbf{v}_k^0)^* \right) \\ &= \sum_{l=1}^L \sum_{k=1}^L \bar{u}_{li} \bar{u}_{kj}^* (\mathbf{v}_l^0 \odot (\mathbf{v}_k^0)^*), \end{aligned} \quad (37)$$

which indicates that $\mathbf{x} \in \mathbb{R}^N$ satisfying $\mathbf{x}^T (\mathbf{v}_i^0 \odot (\mathbf{v}_j^0)^*) = 0, \forall 1 \leq i, j \leq L$, must also satisfy $\mathbf{x}^T (\mathbf{v}_i \odot \mathbf{v}_j^*) = 0, \forall 1 \leq i, j \leq L$, due to the linearity. By Lemma 2, we can conclude that $\mathbf{x}^T \mathbf{J}(\gamma^0) \mathbf{x} = 0$ implies $\mathbf{x}^T \mathbf{J}(\gamma) \mathbf{x} = 0$ for any $\gamma \geq 0$. ■

We now show the necessity of $\mathcal{N} \cap \mathcal{C} = \{\mathbf{0}\}$ for the local identifiability, using contradiction. Suppose that there exists a non-zero vector $\mathbf{x} \in \mathcal{N} \cap \mathcal{C}$. Since $\mathbf{x} \in \mathcal{N}$, we must have $\mathbf{x}^T \mathbf{J}(\gamma^0) \mathbf{x} = 0$. By plugging (8) into $\mathbf{x}^T \mathbf{J}(\gamma^0) \mathbf{x}$, we get

$$\mathbf{x}^T \mathbf{J}(\gamma^0) \mathbf{x} = \mathbb{E} \left[\sum_i \frac{\partial \log p(\mathbf{Y}|\gamma)}{\partial \gamma_i} x_i \right]_{\gamma=\gamma^0}^2 = 0. \quad (38)$$

By noting that the term inside the expectation is nonnegative, we get

$$\sum_i \left(\frac{\partial \log p(\mathbf{Y}|\gamma)}{\partial \gamma_i} \Big|_{\gamma=\gamma^0} \right) x_i = 0. \quad (39)$$

Consider now γ in the neighborhood of γ^0 along the direction \mathbf{x} . Since $\mathbf{x} \in \mathcal{C}$, we must have that γ remains feasible. Now by Lemma 3, $\mathbf{x}^T \mathbf{J}(\gamma^0) \mathbf{x} = \mathbf{x}^T \mathbf{J}(\gamma) \mathbf{x} = 0$, we can repeat the same argument as in (38)-(39) to show that $\sum_i \frac{\partial \log p(\mathbf{Y}|\gamma)}{\partial \gamma_i} x_i = 0$. This means that the directional derivative of $\log p(\mathbf{Y}|\gamma)$ along \mathbf{x} is zero, which implies that $\log p(\mathbf{Y}|\gamma)$ stays unchanged when γ moves from γ^0 along the direction \mathbf{x} in the neighborhood of γ^0 . This implies that γ^0 is not locally identifiable.

To show the sufficiency of $\mathcal{N} \cap \mathcal{C} = \{\mathbf{0}\}$ for the local identifiability, we also use contradiction. Suppose that the local identifiability is not satisfied. This implies that there exists a sequence $\{\gamma^1, \gamma^2, \dots\}$ approaching γ^0 in the feasible neighborhood of γ^0 satisfying $p(\mathbf{Y}|\gamma^1) = p(\mathbf{Y}|\gamma^2) = \dots = p(\mathbf{Y}|\gamma^0)$ for all \mathbf{Y} . We can then construct an infinite sequence of unit vectors $\left\{ \frac{\gamma^1 - \gamma^0}{\|\gamma^1 - \gamma^0\|_2}, \frac{\gamma^2 - \gamma^0}{\|\gamma^2 - \gamma^0\|_2}, \dots \right\}$, which must contain a limit vector due to the fact that the sequence is bounded. Let \mathbf{x} denote this limit vector. By the mean value theorem, for all $n = 1, 2, \dots$, there exists $\bar{\gamma}^n$ between γ^n and γ^0 , such that

$$\begin{aligned} \frac{\log p(\mathbf{Y}|\gamma^n) - \log p(\mathbf{Y}|\gamma^0)}{\|\gamma^n - \gamma^0\|_2} &= \sum_i \frac{\partial \log p(\mathbf{Y}|\gamma)}{\partial \gamma_i} \Big|_{\gamma=\bar{\gamma}^n} \left(\frac{\gamma_i^n - \gamma_i^0}{\|\gamma^n - \gamma^0\|_2} \right). \end{aligned}$$

But $p(\mathbf{Y}|\gamma^1) = p(\mathbf{Y}|\gamma^2) = \dots = p(\mathbf{Y}|\gamma^0)$, which means that the above equation is actually zero for all n . Hence, for the limit vector \mathbf{x} of the sequence $\left\{ \frac{\gamma^1 - \gamma^0}{\|\gamma^1 - \gamma^0\|_2}, \frac{\gamma^2 - \gamma^0}{\|\gamma^2 - \gamma^0\|_2}, \dots \right\}$, we must have

$$\sum_i \left(\frac{\partial \log p(\mathbf{Y}|\gamma)}{\partial \gamma_i} \Big|_{\gamma=\gamma^0} \right) x_i = 0. \quad (40)$$

Note that (40) holds for all \mathbf{Y} . By taking the expectation of its square, we get an equation identical to (38), which implies that $\mathbf{J}(\gamma^0) \mathbf{x} = \mathbf{0}$ by using the positive semidefiniteness of $\mathbf{J}(\gamma^0)$. Therefore, $\mathbf{x} \in \mathcal{N}$. In the meanwhile, since the sequence approaches γ^0 in the feasible neighborhood, we must have $\gamma_i^n - \gamma_i^0 \geq 0$ for all $i \in \mathcal{I}$, as $\gamma_i^0 = 0, i \in \mathcal{I}$, and $\gamma_i^n \geq 0, i \in \mathcal{I}$. Thus, the vectors in the sequence $\left\{ \frac{\gamma^1 - \gamma^0}{\|\gamma^1 - \gamma^0\|_2}, \frac{\gamma^2 - \gamma^0}{\|\gamma^2 - \gamma^0\|_2}, \dots \right\}$ are all unit vectors in \mathcal{C} . This means that the limit vector \mathbf{x} must also be a unit vector in \mathcal{C} , because the intersection of the unit sphere and \mathcal{C} is a closed set. Thus we have that $\mathbf{x} \in \mathcal{N} \cap \mathcal{C}$, and therefore $\mathcal{N} \cap \mathcal{C} \neq \{\mathbf{0}\}$.

Finally, we show that the local identifiability of the true parameter γ^0 is equivalent to the global identifiability of γ^0 for the problem under consideration. Since the global identifiability already implies the local identifiability, we only need to prove that the local identifiability also implies the global identifiability. In the following, we use contradiction to show that if γ^0 is not globally identifiable, then γ^0 is not locally identifiable. Suppose that there exists another $\gamma' \neq \gamma^0$ in $[0, +\infty)^N$ such that $p(\mathbf{Y}|\gamma') = p(\mathbf{Y}|\gamma^0)$. Since both $p(\mathbf{Y}|\gamma')$ and $p(\mathbf{Y}|\gamma^0)$ are zero-mean multivariate Gaussian distributions, the corresponding covariance matrices, denoted by $\Sigma' \triangleq \sum_{n=1}^N \gamma'_n \mathbf{s}_n \mathbf{s}_n^H + \sigma_w^2 \mathbf{I}$ and $\Sigma^0 \triangleq \sum_{n=1}^N \gamma_n^0 \mathbf{s}_n \mathbf{s}_n^H + \sigma_w^2 \mathbf{I}$ from (2) must be identical if their distribution functions are the same, implying

$$\sum_{n=1}^N (\gamma'_n - \gamma_n^0) \mathbf{s}_n \mathbf{s}_n^H = \mathbf{0}. \quad (41)$$

Then, we can construct another $\gamma'' \triangleq \gamma^0 + t(\gamma' - \gamma^0)$ with $t \in (0, 1)$ such that $p(\mathbf{Y}|\gamma'') = p(\mathbf{Y}|\gamma^0)$, since its corresponding mean would be zero and its covariance matrix would also be identical. Note that the positive scalar t can be arbitrarily small, which implies that we can construct such γ'' in any neighborhood of γ^0 , and thus γ^0 is not locally identifiable. This completes the proof of Theorem 2.

C. Proof of Theorem 3

Let $\mathbf{z} \in \mathbb{R}^N$ be a non-zero vector in the null space of $\mathbf{J}(\gamma^0)$, i.e., $\mathbf{J}(\gamma^0) \mathbf{z} = \mathbf{0}$. Since $\mathbf{J}(\gamma^0)$ is symmetric, by rearranging the columns and rows of $\mathbf{J}(\gamma^0)$ and the entries of \mathbf{z} according to the index sets \mathcal{I} and \mathcal{I}^c , the equation $\mathbf{J}(\gamma^0) \mathbf{z} = \mathbf{0}$ can be rewritten in a block-wise form as

$$\begin{bmatrix} \mathbf{A} & \mathbf{B} \\ \mathbf{B}^T & \mathbf{C} \end{bmatrix} \begin{bmatrix} \mathbf{z}_{\mathcal{I}} \\ \mathbf{z}_{\mathcal{I}^c} \end{bmatrix} = \begin{bmatrix} \mathbf{0} \\ \mathbf{0} \end{bmatrix}, \quad (42)$$

where \mathbf{A} , \mathbf{B} , and \mathbf{C} are submatrices of $\mathbf{J}(\gamma^0)$ defined in the theorem, and $\mathbf{z}_{\mathcal{I}} \in \mathbb{R}^{N-K}$, $\mathbf{z}_{\mathcal{I}^c} \in \mathbb{R}^K$ are sub-vectors of \mathbf{z} with indices from \mathcal{I} and \mathcal{I}^c , respectively. We rewrite (42) as

$$\mathbf{A} \mathbf{z}_{\mathcal{I}} + \mathbf{B} \mathbf{z}_{\mathcal{I}^c} = \mathbf{0}, \quad (43)$$

$$\mathbf{B}^T \mathbf{z}_{\mathcal{I}} + \mathbf{C} \mathbf{z}_{\mathcal{I}^c} = \mathbf{0}. \quad (44)$$

We first show that \mathbf{C} is invertible if $\mathcal{N} \cap \mathcal{C} = \{\mathbf{0}\}$. Suppose that \mathbf{C} is singular, i.e., there exists a non-zero vector $\mathbf{v} \in \mathbb{R}^K$ such that $\mathbf{C}\mathbf{v} = \mathbf{0}$. We then construct a non-zero vector \mathbf{z} with $\mathbf{z}_{\mathcal{I}^c} = \mathbf{v}$ and $\mathbf{z}_{\mathcal{I}} = \mathbf{0}$. It can be verified from (42) that \mathbf{z} satisfies $\mathbf{z}^T \mathbf{J}(\gamma^0) \mathbf{z} = 0$, based on which we get $\mathbf{J}(\gamma^0) \mathbf{z} = \mathbf{0}$ by using the positive semidefiniteness of $\mathbf{J}(\gamma^0)$. Therefore, $\mathbf{z} \in \mathcal{N}$. Moreover, the constructed \mathbf{z} is also in the cone \mathcal{C} since $z_i = 0, i \in \mathcal{I}$. Therefore, $\mathbf{z} \in \mathcal{N} \cap \mathcal{C}$. The condition $\mathcal{N} \cap \mathcal{C} = \{\mathbf{0}\}$ is not satisfied, since $\mathbf{z} \neq \mathbf{0}$.

With invertible \mathbf{C} , we eliminate $\mathbf{z}_{\mathcal{I}^c}$ in (43) and (44), and obtain the following equation

$$(\mathbf{A} - \mathbf{B}\mathbf{C}^{-1}\mathbf{B}^T)\mathbf{z}_{\mathcal{I}} = \mathbf{0}. \quad (45)$$

Since the cone constraints are on the coordinates indexed by \mathcal{I} , to check whether $\mathcal{N} \cap \mathcal{C} = \{\mathbf{0}\}$ holds, we only need to examine if there exists a non-zero vector $\mathbf{z}_{\mathcal{I}}$ with nonnegative entries that satisfies (45). Note that we require $\mathbf{z}_{\mathcal{I}} \neq \mathbf{0}$ to make \mathbf{z} non-zero due to (44) and the invertibility of \mathbf{C} . Based on (45), the existence of a non-zero vector $\mathbf{z}_{\mathcal{I}}$ can be formulated as a feasibility problem as follows

$$\text{find } \mathbf{x} \quad (46a)$$

$$\text{subject to } (\mathbf{A} - \mathbf{B}\mathbf{C}^{-1}\mathbf{B}^T)\mathbf{x} = \mathbf{0} \quad (46b)$$

$$\mathbf{x} \geq \mathbf{0}, \mathbf{x} \neq \mathbf{0}. \quad (46c)$$

To get (13) from (46), we use the following lemma from [43].

Lemma 4: Let \mathbf{M} be any matrix over some field. Then, the following statements are equivalent: (i) $\mathbf{M}\mathbf{x} = \mathbf{0}$ has no solution for $\mathbf{x} \geq \mathbf{0}$ and $\mathbf{x} \neq \mathbf{0}$; (ii) $\mathbf{M}^T \mathbf{v} > \mathbf{0}$ has solutions.

By using Lemma 4 and noting that $\mathbf{A} - \mathbf{B}\mathbf{C}^{-1}\mathbf{B}^T$ is symmetric, the infeasibility of (46) is equivalent to the feasibility of (13).

D. Proof of Theorem 4

The proof is based on [44], which considers the case of non-singular Fisher information matrix. Here, we consider the case when Fisher information matrix may be singular. Let $F_M(\gamma)$ denote the log-likelihood function normalized by M , i.e.,

$$F_M(\gamma) \triangleq \frac{1}{M} \log p(\mathbf{Y}|\gamma) = \frac{1}{M} \sum_{m=1}^M \log p(\mathbf{y}_m|\gamma). \quad (47)$$

Since $\hat{\gamma}$ is obtained by maximizing $F_M(\gamma)$, and $\hat{\gamma}$ converges to the true parameter γ^0 as $M \rightarrow \infty$, we study the function $\Delta F(\gamma) \triangleq F_M(\gamma) - F_M(\gamma^0)$ for large M in the neighborhood of γ^0 . Let $\Delta\gamma \triangleq \gamma - \gamma^0$. We consider the quadratic approximation of $\Delta F(\gamma)$ at γ^0 as

$$\Delta F(\gamma) \approx \Delta\gamma^T \nabla F_M(\gamma^0) + \frac{1}{2} \Delta\gamma^T \nabla^2 F_M(\gamma^0) \Delta\gamma, \quad (48)$$

where $\nabla F_M(\gamma^0)$ and $\nabla^2 F_M(\gamma^0)$ represent the gradient and the Hessian of $F_M(\gamma)$ at γ^0 , respectively.

We now aim to relate the gradient and the Hessian to the associated Fisher information matrix. For the gradient term in (48), the i -th entry of $\nabla F_M(\gamma^0)$ can be written as

$$[\nabla F_M(\gamma^0)]_i = \frac{1}{M} \sum_{m=1}^M \left. \frac{\partial \log p(\mathbf{y}_m|\gamma)}{\partial \gamma_i} \right|_{\gamma=\gamma^0}, \quad (49)$$

where each term in the summation can be seen as a random variable with the mean and variance, respectively, as

$$\mathbb{E} \left[\left. \frac{\partial \log p(\mathbf{y}_m|\gamma)}{\partial \gamma_i} \right|_{\gamma=\gamma^0} \right] = 0, \quad (50)$$

$$\text{var} \left[\left. \frac{\partial \log p(\mathbf{y}_m|\gamma)}{\partial \gamma_i} \right|_{\gamma=\gamma^0} \right] = \frac{1}{M} [\mathbf{J}(\gamma_0)]_{ii}. \quad (51)$$

The mean expression in (50) is obtained by taking the expectation of (30) using $\mathbb{E}[\hat{\Sigma}] = \Sigma$, and the variance expression (51) is obtained based on (8) and (50). In particular, notice from (8) that

$$\begin{aligned} [\mathbf{J}(\gamma)]_{ii} &= \mathbb{E} \left[\left(\sum_{m=1}^M \frac{\partial \log p(\mathbf{y}_m|\gamma)}{\partial \gamma_i} \right)^2 \right] \\ &= M \mathbb{E} \left[\left(\frac{\partial \log p(\mathbf{y}_m|\gamma)}{\partial \gamma_i} \right)^2 \right], \end{aligned} \quad (52)$$

where the last step is due to (50) and the fact that \mathbf{y}_m 's are i.i.d. Gaussian random variables conditioned on γ . This shows that (51) holds. Similarly, the covariance can be computed as

$$\mathbb{E} \left[\left(\frac{\partial \log p(\mathbf{y}_m|\gamma)}{\partial \gamma_i} \right) \left(\frac{\partial \log p(\mathbf{y}_m|\gamma)}{\partial \gamma_j} \right) \Big|_{\gamma=\gamma^0} \right] = \frac{[\mathbf{J}(\gamma_0)]_{ij}}{M}. \quad (53)$$

Thus, $\nabla F_M(\gamma^0)$ in (49) is the sample average of M i.i.d. random vectors, whose mean, variance, and covariance are given in (50), (51), and (53), respectively. By the central limit theorem, $\sqrt{M} \nabla F_M(\gamma^0)$ tends to $\mathcal{N}(\mathbf{0}, \mathbf{J}(\gamma^0)/M)$ as M goes to infinity.

For the Hessian term in (48), based on (29) we immediately have that $\nabla^2 F_M(\gamma^0)$ converges to $-\mathbf{J}(\gamma^0)/M$ as M tends to infinity by the law of large numbers.

Now, let $\mathbf{x} \in \mathbb{R}^N$ be a random vector following $\mathcal{N}(\mathbf{0}, M\mathbf{J}^\dagger(\gamma^0))$. Then the random vector $\mathbf{J}(\gamma^0)\mathbf{x}/M$ follows $\mathcal{N}(\mathbf{0}, \mathbf{J}(\gamma^0)/M)$. Therefore, the right hand side of (48), $\Delta\gamma^T \nabla F_M(\gamma^0) + \frac{1}{2} \Delta\gamma^T \nabla^2 F_M(\gamma^0) \Delta\gamma$, converges in distribution to the following random variable

$$\begin{aligned} &\frac{1}{M\sqrt{M}} \Delta\gamma^T \mathbf{J}(\gamma^0) \mathbf{x} - \frac{1}{2M} \Delta\gamma^T \mathbf{J}(\gamma^0) \Delta\gamma \\ &= -\frac{1}{2M} \left(\Delta\gamma - \frac{1}{\sqrt{M}} \mathbf{x} \right)^T \mathbf{J}(\gamma^0) \left(\Delta\gamma - \frac{1}{\sqrt{M}} \mathbf{x} \right) \\ &\quad + \frac{1}{2M^2} \mathbf{x}^T \mathbf{J}(\gamma^0) \mathbf{x}, \end{aligned} \quad (54)$$

where the last step is obtained by completing a square.

Finally, the maximization of $F_M(\gamma)$ is equivalent to the maximization of $\Delta F(\gamma)$ since $F_M(\gamma^0)$ does not depend on γ . Based on (54), the optimization problem can be cast as

$$\text{minimize}_{\Delta\gamma} \left(\frac{\mathbf{x}}{\sqrt{M}} - \Delta\gamma \right)^T \frac{\mathbf{J}(\gamma^0)}{M} \left(\frac{\mathbf{x}}{\sqrt{M}} - \Delta\gamma \right) \quad (55a)$$

$$\text{subject to } \Delta\gamma \in \mathcal{C}, \quad (55b)$$

where $\Delta\gamma \in \mathcal{C}$ comes from the fact that γ should be nonnegative. Replacing $\Delta\gamma$ by $\boldsymbol{\mu}/\sqrt{M}$ completes the proof.

E. Proof of Theorem 5

In the limit $M \rightarrow \infty$, (15) can be written as (16) via vectorization and noting that the sample covariance matrix $\hat{\Sigma}$ converges to the true covariance matrix $\mathbf{S}\mathbf{T}^0\mathbf{S}^H + \sigma_w^2\mathbf{I}$. We prove the necessity of $\tilde{\mathcal{N}} \cap \mathcal{C} = \{\mathbf{0}\}$ by contradiction. We assume that there exists a non-zero vector $\mathbf{x} \in \tilde{\mathcal{N}} \cap \mathcal{C}$. Then we can construct a nonnegative vector $\boldsymbol{\gamma}^1 \triangleq \boldsymbol{\gamma}^0 + t\mathbf{x}$ with $t = \min_{n \in \mathcal{I}^c} (\gamma_n^0 / |x_n|)$. Since $\mathbf{x} \in \mathcal{C}$ and \mathbf{x} is non-zero, it can be verified that $\boldsymbol{\gamma}^1 \geq \mathbf{0}$ and $\boldsymbol{\gamma}^1 \neq \boldsymbol{\gamma}^0$. Moreover, since $\mathbf{x} \in \mathcal{N}$, we have that $\boldsymbol{\gamma}^1$ is also a solution to (16), implying that the condition $\tilde{\mathcal{N}} \cap \mathcal{C} = \{\mathbf{0}\}$ must be necessary.

To show the sufficiency, we also use contradiction. Suppose that there exists a nonnegative vector $\boldsymbol{\gamma}^1 \neq \boldsymbol{\gamma}^0$ such that (16) holds at $\boldsymbol{\gamma}^1$, i.e., $\hat{\mathbf{S}}(\boldsymbol{\gamma}^1 - \boldsymbol{\gamma}^0) = \mathbf{0}$. Let $\mathbf{x} \triangleq \boldsymbol{\gamma}^1 - \boldsymbol{\gamma}^0$. We immediately have $\mathbf{x} \in \tilde{\mathcal{N}}$. In the meanwhile, since $\gamma_n^1, n \in \mathcal{I}$, are nonnegative whereas $\gamma_n^0 = 0, n \in \mathcal{I}$, we have $x_n = \gamma_n^1 - \gamma_n^0 \geq 0, n \in \mathcal{I}$, indicating that $\mathbf{x} \in \mathcal{C}$. Therefore, there exist a non-zero vector $\mathbf{x} \in \tilde{\mathcal{N}} \cap \mathcal{C}$ which contradicts with $\tilde{\mathcal{N}} \cap \mathcal{C} = \{\mathbf{0}\}$, implying that $\tilde{\mathcal{N}} \cap \mathcal{C} = \{\mathbf{0}\}$ is sufficient.

F. Proof of Theorem 6

First, \mathcal{N} is as characterized in Lemma 2 in Appendix B. Let $\mathbf{U}_0, \mathbf{V}_0$, and \mathbf{v}_i^0 denote the values of \mathbf{U}, \mathbf{V} , and \mathbf{v}_i at $\boldsymbol{\gamma}^0$, respectively, as defined in Lemma 2. Note that $\mathbf{V}_0 = \mathbf{S}^H\mathbf{U}_0$. Then, the null set \mathcal{N} is the set of $\mathbf{x} \in \mathbb{R}^N$ that satisfies $\mathbf{x}^T\mathbf{J}(\boldsymbol{\gamma}^0)\mathbf{x} = 0$, which is given by

$$\mathcal{N} = \{\mathbf{x} \mid \mathbf{x}^T(\mathbf{v}_i^0 \odot (\mathbf{v}_j^0)^*) = 0, \mathbf{x} \in \mathbb{R}^N, 1 \leq i, j \leq L\}. \quad (56)$$

Next, we express $\tilde{\mathcal{N}}$ in a form similar to (56). We write $\hat{\mathbf{S}} = [\mathbf{s}_1^* \otimes \mathbf{s}_1, \mathbf{s}_2^* \otimes \mathbf{s}_2, \dots, \mathbf{s}_N^* \otimes \mathbf{s}_N] \in \mathbb{C}^{L^2 \times N}$ explicitly as

$$\hat{\mathbf{S}} = \begin{bmatrix} s_{11}^* \mathbf{s}_1 & s_{12}^* \mathbf{s}_2 & \dots & s_{1N}^* \mathbf{s}_N \\ s_{21}^* \mathbf{s}_1 & s_{22}^* \mathbf{s}_2 & \dots & s_{2N}^* \mathbf{s}_N \\ \vdots & \vdots & \ddots & \vdots \\ s_{L1}^* \mathbf{s}_1 & s_{L2}^* \mathbf{s}_2 & \dots & s_{LN}^* \mathbf{s}_N \end{bmatrix}, \quad (57)$$

from which we observe that the L^2 rows of $\hat{\mathbf{S}}$ can be expressed in the form of $\mathbf{r}_i^T \odot \mathbf{r}_j^H$ for $1 \leq i, j \leq L$, where $\mathbf{r}_i^T \triangleq [s_{i1}, s_{i2}, \dots, s_{iN}]$ is the i -th row of \mathbf{S} . Therefore, the null space $\tilde{\mathcal{N}}$ can be expressed using $\mathbf{r}_i^T \odot \mathbf{r}_j^H$ as follows

$$\tilde{\mathcal{N}} = \{\mathbf{x} \mid \mathbf{x}^T(\mathbf{r}_i \odot \mathbf{r}_j^*) = 0, \mathbf{x} \in \mathbb{R}^N, 1 \leq i, j \leq L\}. \quad (58)$$

We now relate $\tilde{\mathcal{N}}$ in (56) and \mathcal{N} in (58) by noticing that \mathbf{v}_i^0 in (56) and \mathbf{r}_i in (58) are connected via $\mathbf{V}_0 = \mathbf{S}^H\mathbf{U}_0$. Let u_{ij}^0 denote the (i, j) -th entry of \mathbf{U}_0 , based on which \mathbf{v}_i^0 can be written as $\mathbf{v}_i^0 = \sum_{l=1}^L u_{li}^0 \mathbf{r}_l^*$. We then have

$$\begin{aligned} \mathbf{v}_i^0 \odot (\mathbf{v}_j^0)^* &= \left(\sum_{l=1}^L u_{li}^0 \mathbf{r}_l^* \right) \odot \left(\sum_{k=1}^L (u_{kj}^0)^* \mathbf{r}_k \right) \\ &= \sum_{l=1}^L \sum_{k=1}^L u_{li}^0 (u_{kj}^0)^* (\mathbf{r}_l^* \odot \mathbf{r}_k). \end{aligned} \quad (59)$$

Similarly, we have $\mathbf{S}^H = \mathbf{V}_0\mathbf{U}_0^H$ since \mathbf{U}_0 is unitary, and \mathbf{r}_i can be written as $\mathbf{r}_i = \sum_{l=1}^L u_{il}^0 \mathbf{v}_l^*$, based on which we get

$$\mathbf{r}_i \odot \mathbf{r}_j^* = \sum_{l=1}^L \sum_{k=1}^L u_{il}^0 (u_{jk}^0)^* ((\mathbf{v}_l^0)^* \odot \mathbf{v}_k^0). \quad (60)$$

We observe from (59) and (60) that any vector \mathbf{x} that satisfies $\mathbf{x}^T(\mathbf{v}_i^0 \odot (\mathbf{v}_j^0)^*) = 0$ for all $1 \leq i, j \leq L$ should also satisfy $\mathbf{x}^T(\mathbf{r}_i \odot \mathbf{r}_j^*) = 0, 1 \leq i, j \leq L$, and vice versa. Therefore, the two sets \mathcal{N} and $\tilde{\mathcal{N}}$ are identical, implying that $\tilde{\mathcal{N}} \cap \mathcal{C} = \{\mathbf{0}\}$ and $\mathcal{N} \cap \mathcal{C} = \{\mathbf{0}\}$ are equivalent.

G. Proof of Theorem 7

The set of the rows of $\hat{\mathbf{S}}$ can be expressed as $\{\mathbf{r}_i^T \odot \mathbf{r}_j^H, 1 \leq i, j \leq L\}$ from (57). Since $\mathbf{r}_i^T \odot \mathbf{r}_j^H$ is complex, the real and imaginary parts of $\mathbf{r}_i^T \odot \mathbf{r}_j^H$ can be expressed as $\text{Re}(\mathbf{r}_i^T \odot \mathbf{r}_j^H) = \text{Re}(\mathbf{r}_i^T) \odot \text{Re}(\mathbf{r}_j^H) + \text{Im}(\mathbf{r}_i^T) \odot \text{Im}(\mathbf{r}_j^H)$ and $\text{Im}(\mathbf{r}_i^T \odot \mathbf{r}_j^H) = \text{Re}(\mathbf{r}_i^T) \odot \text{Im}(\mathbf{r}_j^H) - \text{Im}(\mathbf{r}_i^T) \odot \text{Re}(\mathbf{r}_j^H)$. We then rewrite $\hat{\mathbf{S}}\mathbf{x} = \mathbf{0}$ as $\mathbf{D}\mathbf{x} = \mathbf{0}$, where \mathbf{D} is a real matrix constructed by $\text{Re}(\mathbf{r}_i^T \odot \mathbf{r}_j^H), 1 \leq i \leq j \leq L$, and $\text{Im}(\mathbf{r}_i^T \odot \mathbf{r}_j^H), 1 \leq i < j \leq L$. If there exists a vector \mathbf{x} that satisfies (21b), (21c), and (21d), we have $\mathbf{x} \in \tilde{\mathcal{N}} \cap \mathcal{C}$. Conversely, if there exists a non-zero vector $\mathbf{x} \in \tilde{\mathcal{N}} \cap \mathcal{C}$, then \mathbf{x} satisfies the constraints (21b) and (21d). We can find a scalar t such that $t\mathbf{x}$ satisfies all (21b), (21c), and (21d).

H. Proof of Theorem 8

The proof is based on the robust ℓ_2 NSP of $\hat{\mathbf{S}}$ established in Lemma 1. Suppose that $\hat{\mathbf{S}}$ has the robust ℓ_2 NSP of order K with parameters $0 < \rho < 1$ and τ under the conditions specified in Lemma 1. As indicated in [45, Sec. 4.3], $\hat{\mathbf{S}}$ also satisfies the robust ℓ_1 NSP of order K , expressed as

$$\|\mathbf{x}_{\mathcal{K}}\|_1 \leq \rho \|\mathbf{x}_{\mathcal{K}^c}\|_1 + \sqrt{K}\tau \|\hat{\mathbf{S}}\mathbf{x}\|_2, \quad (61)$$

by using $\|\mathbf{x}_{\mathcal{K}}\|_1 \leq \sqrt{K}\|\mathbf{x}_{\mathcal{K}}\|_2$ on (23). Consider an \mathbf{x} in the null space of $\hat{\mathbf{S}}$, i.e., $\mathbf{x} \in \tilde{\mathcal{N}}$. Based on (61), we get

$$\|\mathbf{x}_{\mathcal{K}}\|_1 \leq \rho \|\mathbf{x}_{\mathcal{K}^c}\|_1. \quad (62)$$

This condition must be satisfied for any $\mathbf{x} \in \tilde{\mathcal{N}}$ and any index set \mathcal{K} with $|\mathcal{K}| \leq K$.

Now, suppose that $\mathbf{x} \in \tilde{\mathcal{N}} \cap \mathcal{C}$. First, we observe from (57) that the L^2 rows of $\hat{\mathbf{S}}$ can be expressed in the form of $\mathbf{r}_i^T \odot \mathbf{r}_j^H$ for $1 \leq i, j \leq L$, and therefore $\sum_{i=1}^L \mathbf{r}_i^T \odot \mathbf{r}_i^H$ is in the row space of $\hat{\mathbf{S}}$. So, any $\mathbf{x} \in \tilde{\mathcal{N}}$ should satisfy

$$0 = \left(\sum_{i=1}^L \mathbf{r}_i^T \odot \mathbf{r}_i^H \right) \mathbf{x} = \sum_{i=1}^L \sum_{j=1}^N x_j s_{ij} s_{ij}^* = L \sum_{j=1}^N x_j, \quad (63)$$

where the last step is obtained by swapping the summation and noticing that the columns of $\hat{\mathbf{S}}$ share identical ℓ_2 norm since all columns are drawn from a sphere in \mathbb{C}^L . By breaking the summation in the right hand side of (63) into two parts according to \mathcal{I} and \mathcal{I}^c , we have

$$\sum_{i \in \mathcal{I}} x_i = - \sum_{i \in \mathcal{I}^c} x_i \leq \|\mathbf{x}_{\mathcal{I}^c}\|_1. \quad (64)$$

Since $\mathbf{x} \in \mathcal{C}$ also holds, this means that x_i 's, $i \in \mathcal{I}$, are nonnegative. So, $\sum_{i \in \mathcal{I}} x_i = \|\mathbf{x}_{\mathcal{I}}\|_1$, and therefore

$$\|\mathbf{x}_{\mathcal{I}}\|_1 \leq \|\mathbf{x}_{\mathcal{I}^c}\|_1. \quad (65)$$

This above condition should be satisfied for any $\mathbf{x} \in \tilde{\mathcal{N}} \cap \mathcal{C}$.

Finally, we show that the only $\mathbf{x} \in \tilde{\mathcal{N}} \cap \mathcal{C}$ that can satisfy (62) is the zero vector. This is because we can choose \mathcal{K} in (62) to be \mathcal{I}^c since $|\mathcal{I}^c| = K$. In this case, (62) implies

$$\|\mathbf{x}_{\mathcal{I}^c}\|_1 \leq \rho \|\mathbf{x}_{\mathcal{I}}\|_1, \quad (66)$$

while $\mathbf{x} \in \tilde{\mathcal{N}} \cap \mathcal{C}$ implies (65). Noting that $\rho < 1$, the only \mathbf{x} that can satisfy both (65) and (66) is $\mathbf{x} = \mathbf{0}$. This shows that if $\hat{\mathbf{S}}$ has the robust ℓ_2 NSP, then $\tilde{\mathcal{N}} \cap \mathcal{C} = \{\mathbf{0}\}$.

REFERENCES

- [1] Z. Chen, F. Sahrabi, Y.-F. Liu, and W. Yu, "Covariance based joint activity and data detection for massive random access with massive MIMO," in *Proc. IEEE Int. Conf. Commun. (ICC)*, Shanghai, China, May 2019, pp. 1–6.
- [2] Z. Chen and W. Yu, "Phase transition analysis for covariance based massive random access with massive MIMO," in *Proc. 53th Asilomar Conf. Signals Syst. Comput.*, Pacific Grove, CA, USA, Nov. 2019, pp. 1–5.
- [3] M. Hasan, E. Hossain, and D. Niyato, "Random access for machine-to-machine communication in LTE-advanced networks: Issues and approaches," *IEEE Commun. Mag.*, vol. 51, no. 6, pp. 86–93, June 2013.
- [4] C. Bockelmann, N. Pratas, H. Nikopour, K. Au, T. Svensson, C. Stefanovic, P. Popovski, and A. Dekorsy, "Massive machine-type communications in 5G: Physical and MAC-layer solutions," *IEEE Commun. Mag.*, vol. 54, no. 9, pp. 59–65, Sept. 2016.
- [5] L. Liu, E. G. Larsson, W. Yu, P. Popovski, Č. Stefanović, and E. de Carvalho, "Sparse signal processing for grant-free massive connectivity: A future paradigm for random access protocols in the Internet of Things," *IEEE Signal Process. Mag.*, vol. 35, no. 5, pp. 88–99, Sept. 2018.
- [6] E. Dahlman, S. Parkvall, and J. Skold, *4G: LTE/LTE-Advanced for Mobile Broadband*, 2nd ed. Academic press, 2013.
- [7] Z. Dawy, W. Saad, A. Ghosh, J. G. Andrews, and E. Yaacoub, "Toward massive machine type cellular communications," *IEEE Wireless Commun.*, vol. 24, no. 1, pp. 120–128, Feb. 2017.
- [8] Z. Chen, F. Sahrabi, and W. Yu, "Sparse activity detection for massive connectivity," *IEEE Trans. Signal Process.*, vol. 66, no. 7, pp. 1890–1904, Apr. 2018.
- [9] L. Liu and W. Yu, "Massive connectivity with massive MIMO —Part I: Device activity detection and channel estimation," *IEEE Trans. Signal Process.*, vol. 66, no. 11, pp. 2933–2946, June 2018.
- [10] A. Fengler, S. Haghghatshoar, P. Jung, and G. Caire, "Non-Bayesian activity detection, large-scale fading coefficient estimation, and unsourced random access with a massive MIMO receiver," 2019. [Online]. Available: <http://arxiv.org/abs/1910.11266>
- [11] S. Haghghatshoar, P. Jung, and G. Caire, "Improved scaling law for activity detection in massive MIMO systems," in *Proc. IEEE Int. Symp. Inf. Theory (ISIT)*, Vail, CO, USA, June 2018, pp. 381–385.
- [12] A. Fengler, G. Caire, P. Jung, and S. Haghghatshoar, "Massive MIMO unsourced random access," 2019. [Online]. Available: <http://arxiv.org/abs/1901.00828>
- [13] K. Senel and E. G. Larsson, "Grant-free massive MTC-enabled massive MIMO: A compressive sensing approach," *IEEE Trans. Commun.*, vol. 66, no. 12, pp. 6164–6175, Dec. 2018.
- [14] N. Abramson, "The ALOHA system - Another alternative for computer communications," in *Proc. Fall Joint Comput. Conf.*, Houston, TX, USA, Nov. 1970, pp. 281–185.
- [15] E. Casini, R. De Gaudenzi, and O. Del Rio Herrero, "Contention resolution diversity slotted ALOHA (CRDSA): An enhanced random access scheme for satellite access packet networks," *IEEE Trans. Wireless Commun.*, vol. 6, no. 4, pp. 1408–1419, Apr. 2007.
- [16] G. Liva, "Graph-based analysis and optimization of contention resolution diversity slotted ALOHA," *IEEE Trans. Commun.*, vol. 59, no. 2, pp. 477–487, Feb. 2011.
- [17] K. R. Narayanan and H. D. Pfister, "Iterative collision resolution for slotted ALOHA: An optimal uncoordinated transmission policy," in *Proc. Int. Symp. Turbo Codes Iterative Inf. Process. (ISTC)*, Gothenburg, Sweden, Aug. 2012, pp. 136–139.
- [18] E. Paolini, G. Liva, and M. Chiani, "Coded slotted ALOHA: A graph-based method for uncoordinated multiple access," *IEEE Trans. Inf. Theory*, vol. 61, no. 12, pp. 6815–6832, Dec. 2015.
- [19] Y. Han, B. D. Rao, and J. Lee, "Massive uncoordinated access with massive MIMO: A dictionary learning approach," *IEEE Trans. Wireless Commun.*, vol. 19, no. 2, pp. 1320–1332, Feb. 2019.
- [20] J. Wang, Z. Zhang, and L. Hanzo, "Joint active user detection and channel estimation in massive access systems exploiting Reed-Muller sequences," *IEEE J. Sel. Topics Signal Process.*, vol. 13, no. 3, pp. 739–752, June 2019.
- [21] Y. Polyanskiy, "A perspective on massive random-access," in *Proc. IEEE Int. Symp. Inf. Theory (ISIT)*, Aachen, Germany, June 2017, pp. 2523–2527.
- [22] V. K. Amaladinne, A. Vem, D. K. Soma, K. R. Narayanan, and J.-F. Chamberland, "A coupled compressive sensing scheme for uncoordinated multiple access," 2018. [Online]. Available: <http://arxiv.org/abs/1809.04745>
- [23] H. F. Schepker, C. Bockelmann, and A. Dekorsy, "Exploiting sparsity in channel and data estimation for sporadic multi-user communication," in *Proc. Int. Symp. Wireless Commun. Sys. (ISWCS)*, Ilmenau, Germany, Aug. 2013, pp. 1–5.
- [24] V. Boljanović, D. Vukobratović, P. Popovski, and Č. Stefanović, "User activity detection in massive random access: Compressed sensing vs. coded slotted ALOHA," in *Proc. IEEE Workshop Signal Process. Adv. Wireless Commun. (SPAWC)*, Sapporo, Japan, July 2017, pp. 1–6.
- [25] G. Wunder, P. Jung, and C. Wang, "Compressive random access for post-LTE systems," in *Proc. IEEE Int. Conf. Commun. (ICC) Workshops*, Sydney, Australia, June 2014, pp. 539–544.
- [26] X. Xu, X. Rao, and V. K. N. Lau, "Active user detection and channel estimation in uplink CRAN systems," in *Proc. IEEE Int. Conf. Commun. (ICC)*, London, UK, June 2015, pp. 2727–2732.
- [27] J. Ahn, B. Shim, and K. B. Lee, "EP-based joint active user detection and channel estimation for massive machine-type communications," *IEEE Trans. Commun.*, vol. 67, no. 7, pp. 5178–5189, July 2019.
- [28] X. Shao, X. Chen, and R. Jia, "A dimension reduction-based joint activity detection and channel estimation algorithm for massive access," *IEEE Trans. Signal Process.*, vol. 68, no. 1, pp. 420–435, Jan. 2020.
- [29] G. Hannak, M. Mayer, A. Jung, G. Matz, and N. Goertz, "Joint channel estimation and activity detection for multiuser communication systems," in *Proc. IEEE Int. Conf. Commun. (ICC) Workshop*, London, UK, June 2015, pp. 2086–2091.
- [30] Z. Chen and W. Yu, "Massive device activity detection by approximate message passing," in *Proc. IEEE Int. Conf. Acoust., Speech, Signal Process. (ICASSP)*, New Orleans, LA, USA, Mar. 2017, pp. 3514–3518.
- [31] Z. Sun, Z. Wei, L. Yang, J. Yuan, X. Cheng, and L. Wan, "Exploiting transmission control for joint user identification and channel estimation in massive connectivity," *IEEE Trans. Commun.*, vol. 67, no. 9, pp. 6311–6326, Sept. 2019.
- [32] S. Jiang, X. Yuan, X. Wang, C. Xu, and W. Yu, "Joint user identification, channel estimation, and signal detection for grant-free NOMA," 2020. [Online]. Available: <https://arxiv.org/pdf/2001.03930.pdf>
- [33] M. Ke, Z. Gao, Y. Wu, X. Gao, and R. Schober, "Compressive sensing based adaptive active user detection and channel estimation: Massive access meets massive MIMO," 2019. [Online]. Available: <https://arxiv.org/abs/1906.09867>
- [34] Z. Utkovski, O. Simeone, T. Dimitrova, and P. Popovski, "Random access in C-RAN for user activity detection with limited-capacity fronthaul," *IEEE Signal Process. Lett.*, vol. 24, no. 1, pp. 17–21, Jan. 2017.
- [35] Z. Chen, F. Sahrabi, and W. Yu, "Multi-cell sparse activity detection for massive random access: Massive MIMO versus cooperative MIMO," *IEEE Trans. Wireless Commun.*, vol. 18, no. 8, pp. 4060–4074, Aug. 2019.
- [36] D. Donoho, A. Maleki, and A. Montanari, "Message-passing algorithms for compressed sensing," *Proc. Nat. Acad. Sci.*, vol. 106, no. 45, pp. 18 914–18 919, Nov. 2009.
- [37] B. Ottersten, M. Viberg, P. Stoica, and A. Nehorai, "Exact and large sample ML techniques for parameter estimation and detection in array processing," in *Radar Array Processing*, S. S. Haykin, J. Litva, and T. J. Shepherd, Eds. New York: Springer-Verlag, 1993, pp. 99–151.
- [38] D. P. Wipf and B. D. Rao, "An empirical Bayesian strategy for solving the simultaneous sparse approximation problem," *IEEE Trans. Signal Process.*, vol. 55, no. 7, pp. 3704–3716, July 2007.
- [39] S. M. Kay, *Fundamentals of Statistical Signal Processing: Estimation Theory*. Englewood Cliffs, NJ: Prentice-Hall, 1993.
- [40] T. J. Rothenberg, "Identification in parametric models," *Econometrica*, vol. 39, no. 3, pp. 577–591, May 1971.

- [41] A. M. Bruckstein, M. Elad, and M. Zibulevsky, "On the uniqueness of nonnegative sparse solutions to underdetermined systems of equations," *IEEE Trans. Inf. Theory*, vol. 54, no. 11, pp. 4813–4820, Oct. 2008.
- [42] P. Moulin and V. Veeravalli, *Statistical Inference for Engineers and Data Scientists*. Cambridge University Press, 2018.
- [43] A. Ben-Israel, "Notes on linear inequalities, I: The intersection of the nonnegative orthant with complementary orthogonal subspaces," *J. Math. Anal. Appl.*, vol. 9, no. 2, pp. 303–314, 1964.
- [44] S. G. Selfand and K.-Y. Liang, "Asymptotic properties of maximum likelihood estimators and likelihood ratio tests under nonstandard conditions," *J. Am. Stat. Assoc.*, vol. 82, no. 398, pp. 605–610, 1987.
- [45] S. Foucart and H. Rauhut, *A Mathematical Introduction to Compressive Sensing*. Birkhäuser, 2013.